POWER DISTRIBUTION SYSTEM LOSS MINIMIZATION AND VOLTAGE PROFILE IMPROVEMENT USING HARRIS HAWKS OPTIMIZATION TECHNIQUES (CASE STUDY: DEBRE BERHAN POWER DISTRIBUTION SYSTEM)

MASTER OF SCIENCE IN POWER SYSTEM AND ENERGY ENGINEERING

BY

SEID AHMED MUHYE

HAWASSA UNIVERSITY, HAWASSA, ETHIOPIA

FEBRUARY, 2021

POWER DISTRIBUTION SYSTEM LOSS MINIMIZATION AND VOLTAGE PROFILE IMPROVEMENT USING HARRIS HAWKS OPTIMIZATION TECHNIQUES (CASE STUDY: DEBRE BERHAN POWER DISTRIBUTION SYSTEM)

BY

SEID AHMED MUHYE

A THESIS SUBMITTED TO DEPARTEMENT OF ELECTRICAL AND COMPUTER ENGINEERING, HAWASSA INSTITUTE OF TECHNOLOGY, SCHOOL OF GRADUATE STUDIES.

HAWASSA UNIVERSITY

HAWASSA, ETHIOPIA

IN PARTIAL FULFILLMENT OF THE REQUIREMENTS FOR THE DEGREE OF MASTER OF SCIENCE IN POWER SYSTEM AND ENERGY ENGINEERING

FEBRUARY, 2021

HAWASSA UNIVERSITY

INSTITUTE OF TECHNOLOGY

DEPARTMENT OF ELECTRICAL AND COMPUTER ENGINEERING

SCHOOL OF GRADUATE STUDIES

ADVISOR'S APPROVAL SHEET

This is to certify that the thesis entitled "POWER DISTRIBUTION SYSTEM LOSS MINIMIZATION AND VOLTAGE PROFILE IMPROVEMENT USING HARRIS HAWKS OPTIMIZATION TECHNIQUES (CASE STUDY: DEBRE BERHAN POWER DISTRIBUTION SYSTEM) " submitted in partial fulfillment of the requirements for the degree of Masters of Science in Electrical Engineering with specialization in Power system and Energy Engineering, The Graduate Program of the Department of Electrical and Computer Engineering, and has been carried out by Seid Ahmed Muhye ID No- PGPSER/012/10, under my supervision. Therefore, I recommend that the student has fulfilled the requirements and hence hereby can submit the thesis to the department.

Dr. Baseem Khan	.....	.....
Advisor	Signature	Date
Mr. Issaias Giday	.....	.....
Co-advisor	Signature	Date

SCHOOL OF GRADUATE STUDIES

HAWASSA UNIVERSITY

EXAMINER'S APPROVAL SHEET

We the under signed Board of examiners of the final open defense by Seid Ahmed have read and evaluated his thesis entitled " Power Distribution system Loss minimization and Voltage Profile Improvement using Harris Hawks Optimization Techniques (Case Study: Debre Berhan Power Distribution System) and examined the candidate. This is therefore, to certify that the thesis has been accepted in partial fulfilment of the requirements for the degree.

Name	Signature	Date
_____ Chair Person	_____	_____
Dr. Baseem Khan Advisor	_____	_____
Mr. Issaias Gidey Co-advisor	_____	_____
_____ External Eximiner	_____	_____
_____ Internal Examiner I	_____	_____
_____ Internal Examiner II	_____	_____
_____ SGS	_____	_____

Final approval and acceptance of the thesis is contingent upon the submission of the final copy of the thesis to the school of graduate studies (SGS)

Declaration

I, the undersigned, declare that this thesis is my original work, has not been presented for fulfillment of a degree or otherwise in this or any other university, and all sources and materials used for the thesis have been acknowledged. All Advisor's comments are duly incorporated.

Seid Ahmed	.....	.....
Name	Signature	Submission Date

Place: Hawassa, Ethiopia

This thesis has been submitted for examination with my approval as a university advisor.

Dr. Baseem Khan	.....	.....
Advisor	Signature	Date

Acknowledgment

Firstly, it is my pleasure to give special thanks to Allah, the most Gracious, and the most Merciful who is the wonderful source of my strength. He gave me the grace, wisdom, good health and guided me in all the way of my life. Secondly, I would like to acknowledge and extend my deepest gratitude to Dr. Baseem Khan my advisor who offered his support, and encouragement, his valuable and academically essential guidance, hints, motivation, ideas, support and constructive comments were so much beneficial. Throughout this thesis work, I received so much help from him, and completing this thesis work would have been all the most difficult without his support. In addition, he encourages and advising me to engage in research for the future of my life. I would like to acknowledge and extend my gratitude to Mr. Issaias Giday my co-advisor for his essential guidance and motivation and members of electrical staff for their polite, continuous and unmeasurable cooperation by providing me the necessary comments during the thesis progress presentation. I would like to thank also Debre Berhan district utility officials for their sincere cooperation in providing me the necessary data and information. Finally, I would like to thank my families and friends whom I respect and love dearly for their cooperation.

Abstract

Growing concerns over environmental impacts, conditions for improvement of the whole distribution network, shortage and expensiveness of fossil fuel, the deficiency in generating capacities, and ever-increasing demand for electricity have set the way towards distributed generation (DG) units in commercial and domestic electrical power systems. The major problems of distribution systems, such as load growth, power outage, overloaded lines, quality of supply, and reliability can be solved by optimally placing distributed generation near to the customer side. However, the non-optimal placement and size of DG units may lead to high power losses and bad voltage profiles on the power network. This thesis paper aims to minimize system real and reactive power losses, cost and improve the voltage profile of the system by determining the optimal size and penetration of wind-based distributed generation using Harris hawks optimization. The results of base case load flow analysis showed that the case study distribution network feeder has a base case active and reactive power loss of 1629.04KW and 609.513KVAr respectively. The feeder minimum bus voltage and total voltage drop index at the base case is 0.8497V and 0.4407 respectively. The propossed HHO determines the optimal location and size of DG based on minimum loss reduction index, voltage deviation index, and the cost of DG at the same time to use the existing distribution network in an optimal manner. The optimal location of DG is determined to be 33 and 38 with a size of 2.4997MW and 2.4896MW respectively. The active and reactive power loss reduced to 290.097KW and 254KVAr after the DG integration. The method is implemented and tested on the Sheno feeder of the Debre Berhan power distribution system.

Key words: *Distributed Generation, Optimal location, Optimal size, Objective function, technical constraints, loss reduction*

Contents

List of Tables

List of Figures

List of Abberivations

$\%PLR$	Percent of active power loss reduction
$\%QLR$	Percent of ractive power Loss reduction
AEC_{WDG}	Annual Economic Loss with DG
AEC_{WODG}	Annual Economic Loss without any DG
C_{DG}	Cost of DG generated power per kW
L_T	Total DG life in years
P_{DG}	Active Power from Distributed Generation
PL_{WDG}	Active Power Loss with Distributed Generation
PL_{WDG}	Total active power loss after DG installation
PL_{WODG}	Active Power Loss without Distributed Generation
PL_{WODG}	Total active power loss before DG installation
Q_{DG}	Reactive Power from Distributed Generation
QL_{WDG}	Total reactive power loss after DG installation
QL_{WODG}	Total reactive power loss before DG installation
$T\&D$	Transmission and Distribution Systems
TSR	Tip speed ratio
VD_{WDG}	Total voltage drop with DG

VD_{WODG}	Total voltage drop without DG
AC	Alternate Current
ACRI	Annual Cost Reduction Index
CHP	Combined Heat and Power
DC	Direct Current
DFIG	Doubly fed Induction Generator
DG	Distributed generation
GA	Genetic Algorithm
Gbest	Best Global Positio
GHG	Greenhouse House Gas
GSC	Grid side control
HHO	Harris Hawks Optimizer
KVAr	Kilo volt amper
KW	Kilo Watt
LF	Levy flight
MOF	Multi objective Function
MW	Mega Watt
NASA	National Aeronautics and Space Administration
O&M	Operation and Maintenance
Pbest	Best Personal Positio
Pf	power Factor
PL	Active Power Loss

PLRI	Active power loss reduction index
PMSG	Permanent Magnet Synchronous Generator
PSO	Particle Swarm Optimization
PV	Photovoltaic
QL	Reactive Power Loss
QLRI	Reactive power loss reduction index
RDS	Radial Distribution System
RSC	Rotor side control
SLD	Single Line Diagram
VD	Voltage Drop
VDII	Voltage deviation index
WECS	Wind Energy Conversion System

List of Symbols

c_p	Cofficient of power
c_t	Cofficient of torque
E	indicates the escaping energy of the prey
Ed	wind energy density at the site
E_o	the initial state of energy
Et	Energy available at the site
J_g	the generator moment of inertia
J_{total}	The total moment of inertia
J_{turb}	Wind turbine moment of inertia
N	Gear box ratio
T_m	Generator Mechanical Torque
T_{turb}	Turbine torque
T_{em}	GeneratorElectromagnetic Torque
V_m	Average wind speed at reference height
V_w	Available Wind speed at reference height
Z_o	Surface roughness length of the site
λ	Tip speed ratio
ρ	the air density
ω_m	the generator mechanical speed

Chapter 1

Introduction

1.1 Background

In current scenario, the electricity demand grew rapidly due to industrial and domestic needs and conventional energy sources are decreasing rapidly. In the conventional power system, the power transmission carrying capacity has been falling due to increased electricity demand that result in an over-utilized transmission and distribution system with an increased level of losses and higher probability of disturbances. Because of increased demand in the distribution network, the radial distribution lines would be carrying current beyond their maximum capacity, in some cases, at the limit, resulting in increased losses.

There are some conventional methods like Load balancing, bifurcation of overloaded lines, installation of shunt capacitors to reducing the loss in power distribution system. In these types of distribution networks, addition of new loads and supplying the load during interruption becomes very difficult and practically impossible. The thermal loading conditions of the initial sections of the conductors would violate even if there exist a marginal increment in the connected load. Currently in our country there is centralized power system in which there is no any distributed generation near to the load center. With the concern on shortage and expensiveness of resources like fossil fuel and environmental concerns, renewable distributed generation (DG) units such as biomass, wind and solar are emerging as an alternative energy solution. The author in [1] defined distributed generation as the use of any modular electric generation that is sited near the point of use (interconnected to the distribution system) to lower the cost of service.

In general, a distributed generation is nothing but a small-scale power generations that is connected near load center instead of expanding central generation station to minimizing the losses and enhancing voltage stability in power systems [2, 3]. The installation of distributed generation can have either positive or negative impacts [4].Thus, the generators connected in distribution systems in such a manner that it reduce system power loss and operating cost, improve voltage profile, and avoids degradation of power quality and reliability. Along with these assistances, inadequate allocation of DG in terms of its location and capacity may lead to voltage deviation, reduce stability, reliability and power quality, increase line losses, increase system capital and operating costs. The location and capacity of distributed generation units is a complicated optimization issue and should be carefully addressed [5].

The selection of optimal location and size of DG is essential to attain potential benefits with less investment. Recently, many different algorithms have been implemented and proposed to optimally locate and sizing of DG unit. They differ from one another based on the formulation of problem, methodology, constraints and assumptions being made. Network losses are the only objective function considered for determining the optimal allocation of multiple distributed generations using a novel approach method in [6]. The author in [7] have optimally determined the location and the size of PV distributed generation systems particularly for improving voltage support in distribution networks based on particle swarm optimization (PSO). The paper in [8] summerized recent trends of energy usage from renewable sources and reliable operation of hybrid renewable energy system. Maximizing power stability index and minimizing of real power losses considered at the same time to find the global optimal solution for DGs allocation in [9]. A modern interior point method and increasing and replacement strategies are used to obtain the optimal configuration location and sizing of dispersed wind generation to reduce the distribution network loss and improve voltage quality effectively in [10]. The author in [11] studied the detailed analysis of power system reliability with the optimal employment of distributed generation using digital simulation and electrical network calculation program (DIgSILENT). The author in [12] proposed a novel model for DG planning to analyze the influence of DG location and capacity on the probability of protection mal−operation in distribution networks. This paper also considers the minimization of the total cost including DG investment cost, the cost of energy loss, the cost of protection coordination, and

also the mal-operation cost. The authors in [13, 14] use GA and PSO techniques considering short circuit level in the distribution system to find the best location of distributed generations. Moradi and Abedini proposed a hybrid method based on GA–PSO algorithm to find the optimal location and sizing of DG units considering power loss reduction as an objective function within the distribution system [15]. The improved Gravitational Search Algorithm is applied to optimally install and size the renewable distributed generation in a distribution system to minimize the total power losses and average total voltage harmonic distortion [16]. The author in [17] considers the voltage sag as a power quality index to find the optimal allocation of DG units using a genetic algorithm. The paper in [18] also studied the influence of types of DG namely synchronous generation, Wind Turbine and Photovoltaic system on the penetration level and the placement of DG.

Most of the paper above consider only single-objective problems. In this paper, multi-objective Harris hawks optimization technique based on integrating distributed generation is considered and an attempt made to determine the optimal size(s) of DG to minimize real power losses, operating cost of DG, and improve voltage profile in radial distribution systems. The results in this paper have been obtained considering the DGs as Type one (injecting only real power into the system) and as Type two DG providing real and reactive power injection into the system. The annual cost of loss saving due to minimizing the power loss is also calculated and a comparison has been provided.

1.2 Statement of Problem

The electric power consumption in Ethiopia is increasing from time to time due to population growth, industrial growth, social and economic developments whereas supply growth is limitted by exsisting resources, which results in increased current drawn from the source, voltage drop & power loss in the distribution systems. Because of these, power plants are not sufficient to satisfy the people's fundamental services of the country and both utility and connected customers suffer from these loss and voltage drop problems. The people in the Debre Berhan city, which consists of many industry loads, residential and commercial customers, are victims of such problem. Especially for factories and industries, it is really challenging to tolerate such problems since it causes much revenue losses.

Therefore, there must be new system facilities, and improvements in production and use

of electricity to tackle such problems in the power distribution system.
So far different classical methods have been applied to satisfy the load demand, minimize power loss and improve the voltage profile by capacitor placement, conductor upgrading and feeder reconfiguration, tapping cables to the transformers irregularly, and hence overloading and heating is resulted which in turn causes unnecessary power losses. However, it is not a promising approach to solve these problems.

Distributed generation and its integration with the power distribution network is one way of addressing such problems in power systems. However, non-optimal location and sizing of DG units may lead to losses increase together with bad effect on voltage profile of the distribution systems. Therefore, this paper determined the amount of DG penetration and optimum DG placement to minimize the negative impacts and enhance the positive influences of DGs using Harris hawks optimization as it has higher capacity of global convergence, higher diversity, and faster efficiency of searching with minimum operational time .

1.3 Objectives of the thesis

1.3.1 General Objective

- To determine the optimal placement and sizing of DG for optimal operation of the system using Harris hawks optimization for optimizing operation of the distribution system by reducing power loss, cost of DG, and improving voltage profile.

1.3.2 Specific Objectives

- To assess the wind resource availability in the study area
- To identify main cause of power interruption in the feeder
- To determine the maximum possible DG integration with respect to the given constraints
- To compare the results of the system with DG implementations with the present grid

- To draw appropriate conclusions and recommendations from the result of the investigation

1.4 Scope of the thesis

The paper mainly limited on voltage profile improvement and power loss reduction of distribution feeders by optimally locating and sizing DG using optimization techniques. This thesis work mainly includes:

- Steady state analysis of a power distribution system using load flow analysis
- Comparision of system operating parameters with and without distributed generation
- Develop a program for optimal placement and size of the DG in matlab based on Harris hawks optimization techniques for power loss minimization and voltage profile improvements
- Test and compare the program on Debre Berhan radial distribution feeder to confirm its eligibility

1.5 Significance of the thesis

Some of the significance of this thesis paper includes:

- Presence of DGs in the distribution network can extend equipment maintenance intervals, reduce electrical line losses, and improve distribution system reliability and voltage profile, all with cost savings to utilities
- DGs also contribute to the application of competitive energy policies, diversification of energy resources, and reduction of on-peak operating cost, lower losses, lower transmission, and distribution costs
- Useful tool for the utilities for practical implementation of DG

1.6 Motivation for DG

There are mainly three units of electric power system namely production, transmission, and distribution unit and devices that make use of the electricity. The main requirement of the electric power system is to enable power transfer between the generators and the distributing system maintaining an acceptable reliability and voltage quality for all customers (producers and consumers). However, the far distance between the production unit and end-users increase the transmission and distribution loss, interruption duration that reduces optimal operation of the systems. Power engineers find DG motivation and energy producers as both the utility and customers benefits in DG applications in terms of cost and quality supply. The utility invest much cost for the expansion and maintenance of transmission and distribution ($T\&D$) systems, which is a tough and expensive task for utilities. Improvements are regularly necessary to keep up with energy consumption growth.

By employing DG at the distribution level where there is significant growth, cost related to improvements of the equipment size can be avoided while the energy losses related to $T\&D$ can be reduced. Studies can reveal that $T\&D$ costs attributed 30% of those costs that customers pay for electricity [19]. The on-site integration of DG reduce such extra cost on customer due to $T\&D$ costs.

Regarding environmental matters, several of the conventional types of production result in the emission of carbon dioxide with the much-discussed global warming as a very likely consequence. Changing from conventional production based on fossil fuels, such as coal, gas, and oil, to renewable sources, such as sun and wind, would reduce the emission.

1.7 Thesis Outline

This thesis work is structured into six chapters:

Chapter 1 presents the background, problem statements, objectives, and motivation for DG integration. The need to shift the power system to a decentralized power system is explained well in this chapter. It also explains that the location and size of DG have an impact on distribution system operation.

Chapter 2 explains the concept and types of distributed generation (DG), impact of inte-

grating distributed generation into the distribution system. The wind resource assessment are also explained in this chapter.

In chapter 3, different factors and indexes namely the power loss and voltage deviation indexes are formulated to help in solving the optimal location and sizing problem.

The weight factors are used in the formulation of the multi-objective function and the operational constraints are done in this chapter.

In chapter 4, the modeling of wind turbine and DFIG with their respective controller is presented. The MPPT controller for the wind turbine and the vector controlled mechanism for DFIG are implemented.

In chapter 5, the results obtained are presented and analyzed in detail in terms of tables and graphs.

Chapter 6 presents conclusions, recommendations, and future works.

Chapter 2

LITERATURE REVIEW

2.1 Introduction

This chapter presents the definition of distributed generation, types of distributed generation technology, impact of distributed generation, and benefits to the distribution network. There are different definitions of DG in different literature. Distributed generation named as decentralized generation, site generation that generates electrical energy through alternate energy-producing resources close to the customer side to reduce the expansion of the present expensive electric transmission system [20]. In general, the standard definition of distributed generation (DG) is installing small-scale generation units (typically 1KW – 50MW) to produce electricity at different locations tied directly to the distribution substation or near to the load for power flow reduction, loss minimization, voltage profile enhancement and voltage stability improvement [21]. Some of the distributed generators include combustion gas turbines, fuel cells, solar photovoltaic, geothermal, and wind turbines. Usually, distributed generation integration to the distribution system is via power electronic converter or other power electronic devices [22]. When distributed generation integrated into a distribution system, it can have a positive or negative impact on power system operating parameters. Different researchers apply different techniques to get its optimal location and size so that to reduce its negative impact on the distribution system. DG includes both renewable and non-renewable sources which mainly support the increased energy-demand, peak shaving, and to use as a backup generator.

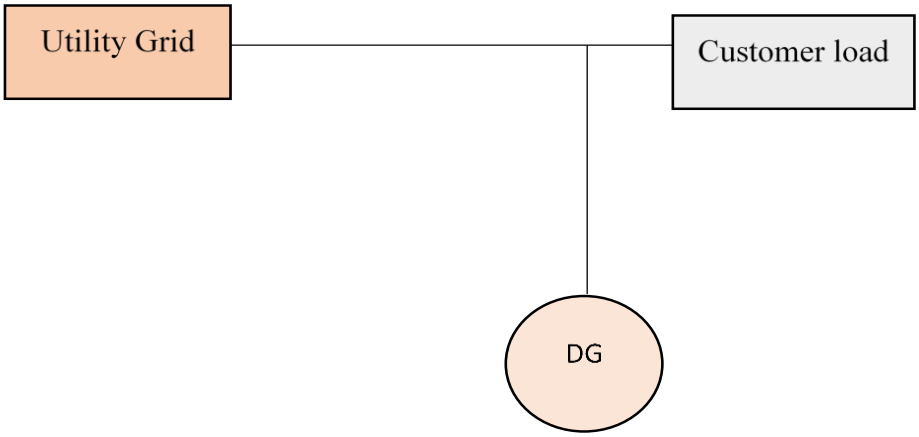

Figure 2.1: Distributed generation definition

2.2 Distributed Generation Technologies

There are two major classifications of distributed generation in the world today applying in power systems. Based on the type of fuel they use for their operation, DGs classified into two groups namely; renewable and non-renewable distributed generation resources. Both of them help the power distribution system to increase the efficiency and reduce the cost of operations, installations, and maintenances.

Non-renewable DG resource: They incorporate technology such as natural gas, coal, gas turbine, microturbine, and petroleum to produce energy for different operations. Mostly used as distributed generations in the areas where the available renewable energy resource is not sufficient for reliable operation. However, the burning of fossil fuels has contributed the largest percentage to global warming, greenhouse gases, acid rain, petrochemical pollution, and eventually run out of use because of the high rate of energy demand and not sustainable and not replaced by a natural means.

Renewable DG technologies: Renewable DG technologies are the electric power generation resources that directly connected to the consumer's load on the distribution systems at the medium voltage or low voltage levels. The renewable DG technologies include geothermal power, biomass, solar power, hydro power, and wind turbines. They provide a technical and economical improvement in power system networks and at the same time to reduce the need to support the increasing demand and reduce CO2 emission.

Commonly used DG technologies are explained below and wind energy system are selected in this paper to implement as distributed generation source in the distribution systems considering the availability around Debre Berhan power distribution systems.

2.2.1 Geothermal Power

Geothermal energy extract heat from the sub-surface of the earth, which originates from radioactive decay of materials or inject water in the case of dry rock technology. The heat generated requires conversion by mechanical means or used directly. The geothermal heat is used faster than it can be recovered by the heat in the center of the earth that makes the production of some geothermal plant in order to dropped siginificantly over time.Production of power from geothermal energy requires wells to access the system to derive turbine connected to electrical generator. The extracted steam pumped through steam pipelines and the kinetic energy of the steam is transformed into rotational mechanical power. The alternator connected to the turbine axis rotates and transforms mechanical rotational energy into electrical energy, which transferred to the distribution network. Not all the steam pumped to the turbine and the steam exits the turbine returned to the liquid state in a condenser. A cooling tower used to cool the water produced from the steam condensation process. The gases that cannot be condensed are dispersed in the atmosphere and the condensed water is then re-injecting it into the deep rock layers [23].

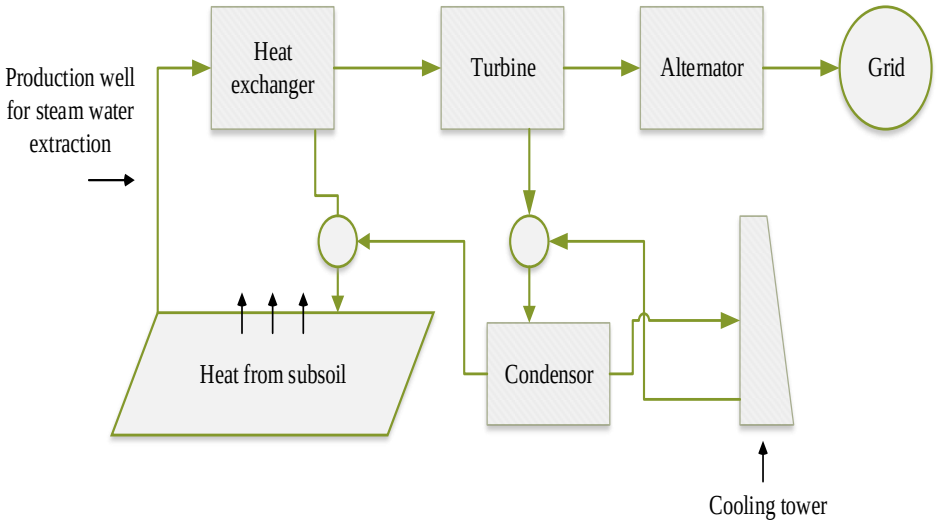

Figure 2.2: Schematic diagram of geothermal energy [23]

2.2.2 Fuel Cell

A fuel cell is an electrochemical cell that generate a fuel through the chemical reaction of hydrogen ions with oxygen without combustion. The electrochemical devices convert the chemical energy of a fuel directly to electricity and heat. The waste heat from fuel cells used for heating applications in low-pressure steam tied into hot water distribution systems. In addition to electrical power generation technology, fuel cells used in CHP applications.

There are several types of fuel cells, but commonly all of them consists of a cathode and an anode separated by an electrolyte that allows ions to move between the two sides of the fuel cells. The fuel (for example, hydrogen or natural gas) supplied to the anode. The second electrode (the cathode) supplied with oxygen by simply pumping air in. Oxidation reactions that generate ions (often positively charged hydrogen ions) and electrons take place at the anode and these ions move through the electrolyte from the anode to the cathode. At the same time, electrons flow through an external circuit from the anode to the cathode, producing direct current electricity. The ions, electrons, and oxygen react with each other at the cathode due to the catalyst in it, forming water and possibly other products [24]. Now the most commercially available type of fuel cell is the proton exchange membrane due to its highest energy density per volume rate.

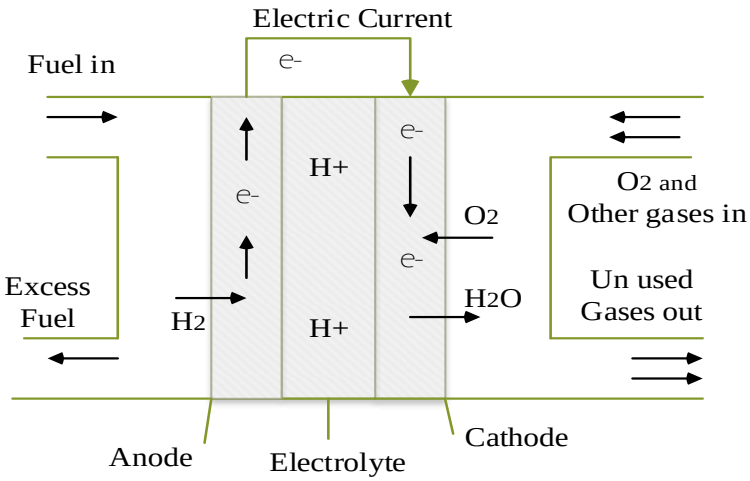

Figure 2.3: Schematic diagram of a fuel cell [24]

2.2.3 Biomass Energy

Biomass is a renewable source of fuel developed from organic materials and a sustainable source of energy like scrap limber, forest debris, certain crops, manure, forest waste, industrial waste, etc. The waste burned to produce steam that runs the turbine to make electricity or that provides heat to industry and home. Biomass converted to electricity directly by combustion to produce heat, or indirectly after converting it to discrete forms of biofuel. In some biomass industries, it used as combined heat and power (CHP) systems in which the extracted or spent steam from the power plant is also used for manufacturing processes or to heat buildings, which greatly increase the overall energy efficiency of the system [25].

Conversion of biomass to biofuel achieved by electrochemical conversion methods, thermal, chemical, and biochemical conversion. On the other hand, it is possible to convert the solid biomass into a fuel gas. Biomass has a valuable contribution to the overall energy supply system mainly because of its very low cost and the fact that it is renewable. There is still considerable scope for making better use of the existing biomass energy supplies and well positioned to play a major role to reduce greenhouse emissions. Biomass has the advantage of controllability and availability compared to other renewable energy when needed. The fuel needs to be delivered, stored, procured, and paid for which is the disadvantage of biomass energy.

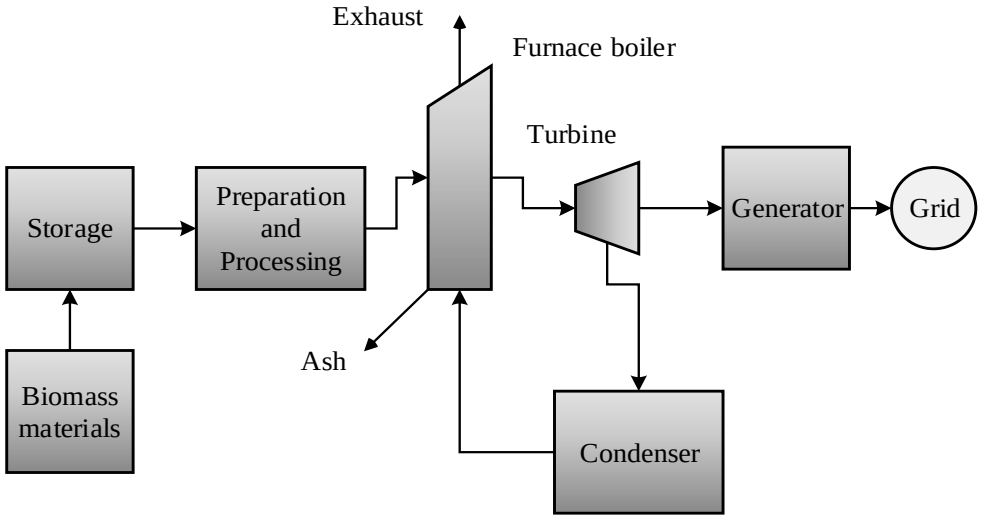

Figure 2.4: Schematic diagram of a biomass energy [25]

2.2.4 Solar Power

The conversion of energy from sunlight into electrical energy with the help of directly using photovoltaic (PV) cell or indirectly using concentrated solar energy called solar power. A solar PV cell is a large-area semiconductor diode consisting of a p-n junction created by doping into the semiconductor crystal. The crystal consists of covalent bonds to the neighboring atoms for the most commonly used silicon solar cells. The location of the sun in the sky and the amount of cloud cover, determine the amount of power produced by a solar power installation. The location of the sun in the sky shows a predictable daily and seasonal variation caused by the rotation of the earth on its axis and around the sun.

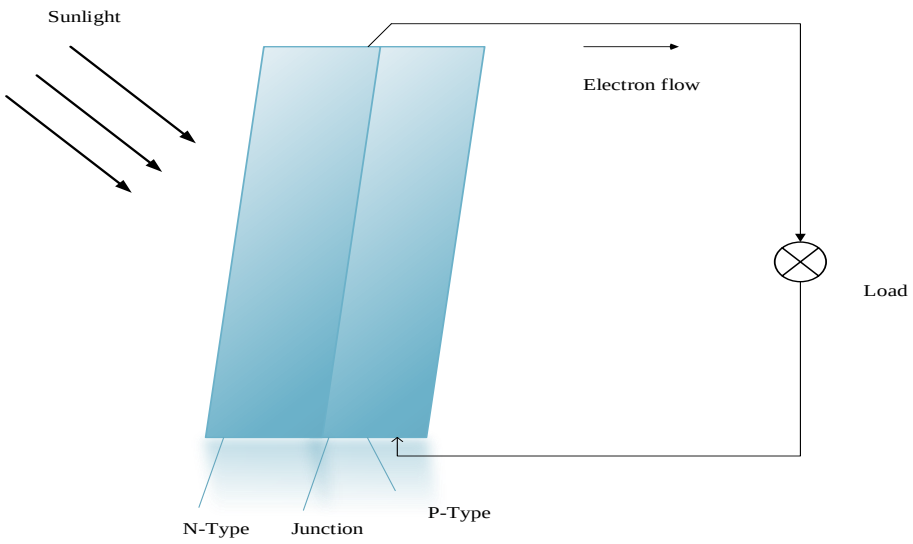

Figure 2.5: Schematic diagram of solar power [26]

The cell generates less amount of DC power, so the PV cells connected in series and parallel to form a module, panel, and array to increase the output of current and voltage in DC. Solar panels is the most widely used, often installed on the roof of a building that only transfers part of the solar energy into electrical energy [27].

2.2.5 Wind Energy System

The wind energy is also a renewable energy that converts kinetic energy from the horizontal displacement of air into kinetic energy of the rotation of a turbine by means of a number of blades to turn the electric generator and traditionally to do other works, like pumping and mining.

The electrical generator then transforms this mechanical rotational energy into electrical energy. The conversion of wind energy to an electrical energy system consists of wind turbines having an aerodynamic rotor, a mechanical transmission system, an electric generator, and a rotor control system. The wind system offers a good power solution because of being cost-effective, low operation and maintenance (O&M) costs, readily available, plentiful, renewable, free, clean, emit no gas such as $Co2$ that makes it growing at a rapid rate, and it is one of the dramatic growing energy source.

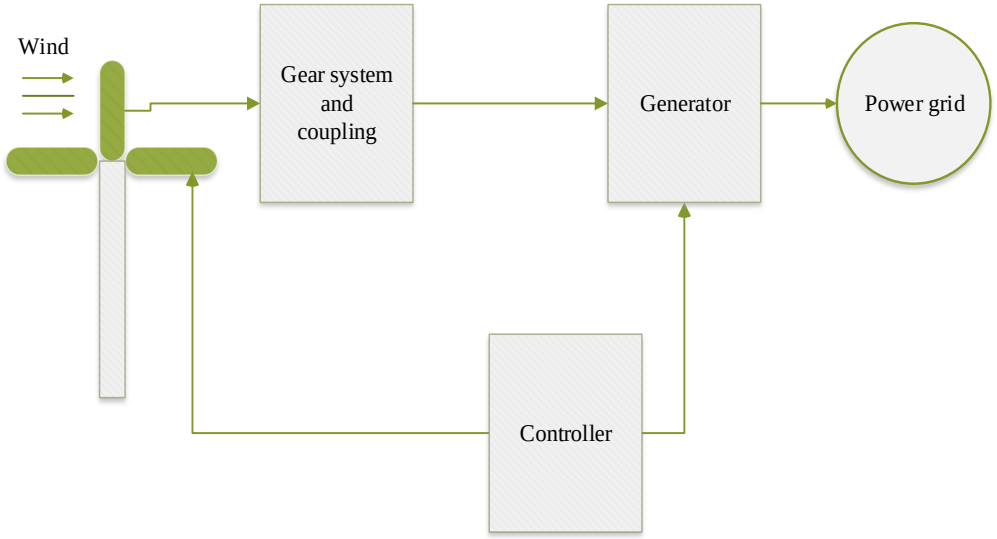

Figure 2.6: Schematic diagram of wind energy system [28]

2.2.5.1 Wind Speed Data of the Site

The available wind speed measured at 10 meters height for Debre Berhan from NASA indicates that wind with minimum speed occurs during August (3.7m/s), while the wind with high velocity occurs during December, November, February, and January; 5.31, 5.28, 5.17, and 5.15m/s respectively. The wind resource data collected for five years at 10m height and the monthly average wind Speed of the Site is given in table 2.1 bellow.

Table 2.1: Monthly Average Wind Speed of the Site

Month	Jan	Feb	Mar	April	May	Jun	July	Aug	Sept	Oct	Nov	Dec	Average
Speed (m/s)	5.15	5.17	5.03	5.09	4.90	4.6	4.07	3.70	4.04	5.24	5.28	5.31	4.81

The table above indicates that the mean wind speed of the month at 10 m height is 4.81m/s.

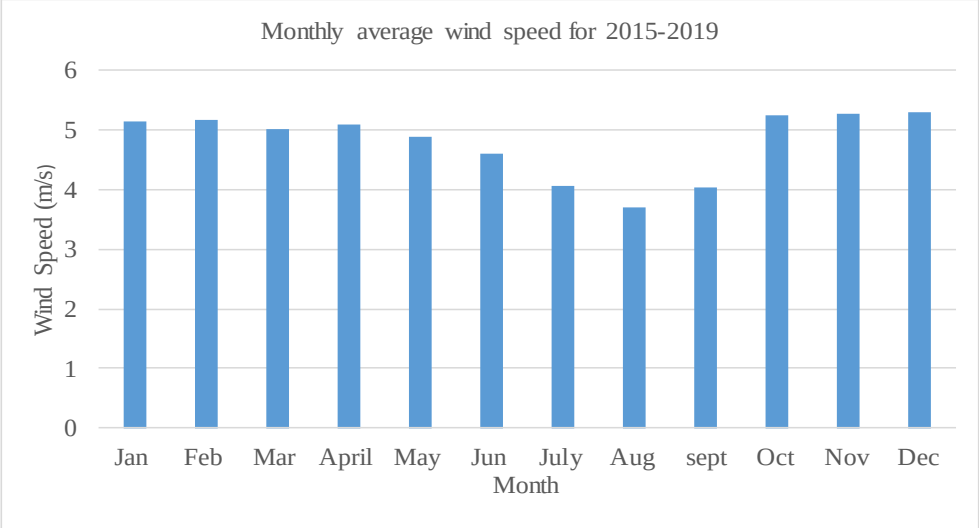

Figure 2.7: Monthly Average Wind Speed of the Site at 10m

The annual average wind speed at 10m for the Debre Berhan site is already known before which is $4.81 m/s$ and the average wind speed at the desired height(h) with the wind shear exponent of Zo is calculated as follows:

$$V_w = V_m \left[\frac{\ln(\frac{h}{z_o})}{\ln(\frac{h_r}{z_o})} \right] \tag{2.1}$$

Where;

V_w = wind velocity at desired height (h)

V_m = average wind speed at reference height (hr)

Z_o = surface roughness length of the site

The annual average wind speed at 10m for the Debre Berhan site is already known before which is 4.81m/s and using equation (2.1) the average wind speed at the desired height of 80m with the wind shear exponent of 0.12 is calculated to be 7.07m/s.‘

2.2.5.2 Power and Energy Estimation by a Wind Turbine Based on Rayleigh Approach

Each wind turbine has a wind speed power curve that describes its own characteristic. The shape of the wind speed power curve is influenced by the wind speed, the blades area, the choice of airfoil, the number of blades, the blade shape, the optimum tip speed ratio,

the speed of rotation, the cut-in wind speed, the shutdown speed, the rated speed, and gearing and generator efficiencies.

Energy produced at any wind speed can be obtained by multiplying the number of hours of its duration by the corresponding turbine power at this wind speed obtained by the turbine's power curve. The total energy produced is calculated by summing the energy produced at all the wind speeds within the operating range of the turbine. Considering Rayleigh distribution, wind energy density at the site is given by the expression:

$$Ed = \left(\frac{3}{\pi}\right) \rho V_m^3 \tag{2.2}$$

Energy available at the site for the unit area of the rotor, over a time can be estimated using the expression:

$$Et = T * Ed = T * \left(\frac{3}{\pi}\right) \rho V_m^3 \tag{2.3}$$

Where;

Ed is wind energy density at the site

Et is Energy available at the site

T is no of hour/month, ρ is the air density

Table 2.2: Wind Energy Potential Based on Rayleigh Analysis at 10 m height

Month	Vm(m/s)	Ed (KW/m2)	Et (KWh/m2)
Jan	5.15	0.157	117
Feb	5.17	0.159	107.7
Mar	5.03	0.146	108.88
April	5.09	0.151	109.2
May	4.9	0.135	100.66
Jun	4.6	0.111	80.594
July	4.07	0.078	57.683
Aug	3.7	0.058	43.338
Sep	4.04	0.075	54.597
Oct	5.24	0.165	123.101
Nov	5.28	0.169	121.879
Dec	5.31	0.172	128.101

From the table 2.2 above, it can be concluded that there is potential wind energy from the site to supply parts of the distribution feeders.

2.3 Impact of Distributed Generation

With an increased number of distributed generation integrated to distributed networks, it leads to some challenges to the network planning. Traditionally, the distribution systems are designed to deliver the electrical power in one direction only from the source to the load direction. When DG installed, it changes the normal characteristics of the distribution system and maximizes green energy penetration in the utility network, increases the concern of voltage and frequency stability [29]. The effect of DG on enhancing power system quality by improving the voltage profile and power loss reduction also investigated. The integration of Distributed generation in radial distribution systems introduces a new source in the system and it causes to change the direction of power flow, which considerably affect the power flow and voltage conditions at both, customers and utility side. The major impacts of integrating distributed generation to power distribution system identified as voltage variations and unbalance, current and voltage harmonics, short circuit level, and other power quality issues, such as flicker and stress on distribution transformer [30]. The distributed generation can affect the system both positively and negatively depends on the operating characteristics of the distribution system and the DG as well. It can also affect the system technically or economically.

2.3.1 Impact of DG on Loss

Normally the real power loss reduction draws more attention for the utility, as it reduces the efficiency of transmitting energy to consumers. The placement of DG along the network feeders can help both the customers and the utility to reduce system loss as it provide both real and reactive power to the system. The integration of DG may increase or decrease the loss in the distribution systems depending on the capacity and location of DG on each part of the distribution network [31]. At the lower penetration of DG, the loss is reduced, however as the penetration increases, the power loss begins to increases. This means there is a maximum penetration level beyond which the DG will increase loss in the network. Locating and sizing the DG units should be as optimum as possible to achieve a better reliability of the system with reduced losses and to reach an optimal performance of the power network. The studies presented the positive effects of the small capacity of DGs on loss reduction when connected to feeders having high losses in the system, and

it is a great benefit for the utilities. Different penetration levels used to determine the impact of increased DG penetration on grid losses. Grid losses decreased at lower DG penetrations and showed an increase in grid losses with increased penetration.

2.3.2 Impact of DG on Voltage Regulation

Voltage regulation is one of the main problems in radial distribution networks. The most common device and techniques used for voltage regulation in the distribution systems are load tap changer transformers, voltage regulators, and shunt capacitors. The penetration of DG in the system changes the power flow of real and reactive power, as well as voltage magnitude, is also changed. These make the Distribution network active and non-unidirectional. Nevertheless, the presence of DG can provide either a positive or negative impact on voltage regulation depending on the characteristic, location, and size of DG [32]. It causes to occur voltage fluctuation and more loss, which are the negative effects of DG but the voltage profile improved well if DG is placed at the optimal location. When the DG unit is beyond 10MW, the impact on the primary feeder is high and then voltage regulation analysis is required to make sure the feeder voltage within suitable limits [33].

2.3.3 Impact of DG on Voltage stability

Always power system required to operate near to its stability limit due to the rapid growth of power demand. However, the entire system operated on the border of the voltage instability region while the voltage profiles of the system are still within the normal operating margins. DG benefits the customers by providing electricity within a short distance between the source and the customer that reduce the measurement of the voltage stability margin (VSM). The study in [34] uses different optimal capacities distributed generation to check the effect on the voltage stability of the system in model of medium voltage meshed distribution system. The result showed that penetration of DG increases the active power injected into the bus and will improve the overall voltage profile and system voltage stability has increased. Distributed generation is a way of improving voltage stability and power loss and maintain steady and acceptable voltage at all buses in the system after subjected to a disturbance from a given initial operating condition. The integration of DG at a feeder provides active power locally and has the potential to provide added reactive power support.

2.3.4 Impact of DG on Power Reliability

Electric power system should continuously supply power to satisfy the customers. This named as reliability. The reliability of the system affected by the placement and control of DG and protection devices with respect to DG penetration [35]. If the penetration is not optimal and the control is not good, the system reliability levels may decline to meet the user demand for power supply, otherwise you can improve the reliability of the distribution network. After DG and power grid, when DG interrupts the power supply unit, the system can compensate for the load in the shortest time difference. The optimal penetration of distributed generation in the distribution system has a positive impact on distribution system reliability. This is due to interruption frequency and interruption duration reduce as the distance between of load point and DG reduces. DG used as a back-up generator when the main power supply in case interrupted. In addition, the distribution network's restoration capability can be improved and give additional capacity to feeders or substations. DG can eliminate network constraints (voltage drop or feeder loading) during the restoration process. The author in [36] showed that reliability of distribution system increases with integrating single DG unit into the distribution system and injecting multiple DG at different locations and near to load points in distribution network further increases reliability of distribution system, while introducing multiple DG at single location improves reliability of distribution system.

2.3.5 Impact of DG on Harmonics

Harmonics are always present in power systems to some extent caused by, for instance, non-linearity in transformer exciting impedance or loads such as fluorescent lights, AC to DC conversion equipment, variable-speed drives, switch-mode power equipment, arc furnaces, and other equipment. The integration of DG produce harmonics in the network either from the generation unit itself (generator) or from the power electronics equipment such as inverters used to transfer the DC power generated from renewable energy to AC to supply the grid. The paper in [37] considers different types of distributed generation (DG) units like a mini-hydro synchronous generator, photovoltaic system, and double fed induction generator wind turbine to analyze harmonic impact in low voltage distribution systems.

Therefore, care should be given to the impact of DG on harmonics and when there exists a worst case in the operation, the equipment at the DG may need to be disconnected to remove the extra heating caused by the harmonics.

2.4 Distributed Generation Benefits

In the centralized way of transmission and distribution system, a large number of residential, commercial, and industrial loads supplied from long distances by large size of sources, which is costly and wastes the electricity because of aging transmission equipment, system outage, and growing congestion. Unlike large central power plants, DG required less investment cost for connecting the source to the load as it installed near the load center by decreasing the distance it travels and the amount that lost with ratings range from 5KW up to 100MW and [38].

Some of the majior benefit drawn through the interconnection of DG units into electric power networks are economic, environmental and technical benefit.

2.4.1 Economic Benefits

The act of integrating DG units closer to the load center leads to avoidance of the need for building new and costly transmission and distribution lines, upgrading the existing power supply system, and reducing transmission and distribution capacity during network planning. Distributed generation sources provide good flexibility and adaptation to the changes in the economic environment due to their short construction lead-time and small size. Moreover, distributed generation technologies can help suppliers to fill in the slots in the liberalized market and provide electricity services as required by the customers. Thus, DG can be a least-cost planning alternative and cause a considerable reduction in required investment cost for supplying increased load in future years [39].

Some economic benefits of DG are as follows:

- DGs can be installed in a very short period at any location as modules and its capacity can be increased or decreased by adding or removing more modules, respectively.
- Lowering cost by avoiding long-distance high voltage transmission and promote competitive markets.

- Distributed generation supply power during peak demand periods (Peak Shaving) which contributes to avoiding electricity price fluctuations and provides a flexible reaction in evaluating electricity prices.

- Provide ancillary services, cost saving by reducing peak demand for central power station and remote power applications.

- DGs satisfy an increase in load growth, by sizing it in small increments.

- Integration of DG reduces power demand from central plant, which reduce the wholesale power price by supplying power to the grid.

- In addition, the planning of DG is a short-term investment approach due to low capital cost and reducing time for installation and hence minimizing investment risk.

- It improve economic benefit by minimizing the number of voltage regulator and capacitor reduce the feeder, power loss and minimizing the cost of loss and by decreasing the loading on electric equipment, minimizing their maintenance cost.

- Running costs more or less constant over the period with the use of renewable sources.

2.4.2 Technical Benefits

Both the utility company and the consumer are benefit from the integration of distributed generation into the utility's conventional resources. DG has an important role in power distribution systems to improve service reliability by reducing the number of system outages and by avoiding line extensions to remote areas. Such systems can also relieve thermal overloads in selected utility distribution systems. Other important benefits also exist, such as loss reduction on both distribution and transmission lines and voltage support. DGs can provide different technical benefits based on different factors, for example, location and technology. The following are some of the technical benefits [40].

- Improving availability and reliability of the power supply network by having a back-up generation.

- Voltage regulation support and Power-loss reduction

- Give benefit to utility system such as system security by diversifying the energy sources and solving power quality problems, such as voltage sags, as the installation of a DG increase the voltage level in the network.

- Reducing power flow inside the transmission network to fit certain constraints and improve its voltage profile

- DGs can help in peak load shaving avoiding problems that might be associated with high demands such as load shedding and transmission line congestion.

- Other benefits of DG include providing ancillary service, and adding self-generation to customer options

2.4.3 Environmental Benefits

The generation of Electric power from large and centralized power plants emit a significant amount of carbon dioxide, sulfur oxide hydrocarbons, and nitrogen oxide, which is a major contributor to climate change. The need to reduce carbon emission into the environment is also to reduce noise pollution and protect other creatures made possible by DG power source. Recent DG technologies offer an environmentally friendly source of electrical energy by limiting the Greenhouse house Gas (GHG) emissions. Distributed generation can also play a role, as it allows optimizing the energy consumption of firms that have a large demand for both heat and electricity [41]. Another benefit of DG is that it reduces the tendency of construction of new transmission circuits and large networks that takes land resource available in the customer's hand.

Based on the above literature, it can be concluded that sufficient work has been conducted with respect to integrating distributed generation in distribution systems. However, the literature reveals that the problem considering power loss, operational cost and voltage profile as a multi objective function as the same time for effective siting and sizing of DG units in distribution networks has not been addressed. In this paper, therefore multi objective based HHO technique adopted to optimize the operation of a distribution system through allocating DG units.

Chapter 3

MODELING AND PROBLEM FORMULATION

These thesis works have mainly two modeling and problem formulation. The first one is mathematical modeling of the load flow analysis of the power system to calculate the optimal size and location of distributed generation. The second one is modeling and formulation of the energy conversion system from the wind (WECS) to generate the determined optimal size of DG from the wind available in the area, which is explained in the next chapter.

3.1 Mathematical Modeling of Load Flow Analysis using Newton Raphson Method

This chapter deals with the problem formulation including the general form of optimization procedure and mathematical formulation of sensitivity factor for power loss, real and reactive power flow using newton raphson method. The multi-objective function is formulated taking into consideration some key factors like real power loss reduction, reactive power loss reduction, and voltage profile improvement index. Both equality and inequality constraints to which the multi-objective function is subjected to are also defined here. For the analysis, considering the single line diagram(SLD) of two buses connected between buses p and q as shown in figure 3.1.

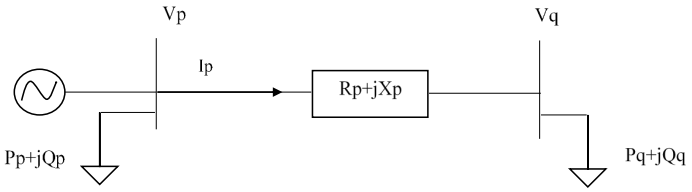

Figure 3.1: Single line diagram of a two bus RDS

Where;

P_P and Q_p is real and reactive power flow at p^{th} bus respectively

P_q and Q_q is real and reactive power flow at q^{th} bus respectively

V_p and V_q is voltage at p^{th} and q^{th} bus respectively

R_p and X_q is resistance and reactance of the line connecting p^{th} bus to q^{th} bus

δ_p and δ_q is power angle at p^{th} bus and q^{th} bus respectively

I_p is current flow in the branch connecting p^{th} bus to q^{th} bus

3.2 System Power Flow Sensitivity Factors

Power flow sensitivity of the power system is the change in power flow in a transmission or distribution line connected between two buses say bus p and bus q due to unit change in the power injected at any buses in the system. Considering the single line diagram above, the complex power injected by a source into a bus of a power system is given by:

$$S_p = P_p + jQ_p = V_p I_p^* \qquad p = 1, 2, 3, \ldots, n \tag{3.1}$$

Where;

V_p is the voltage at the bus with respect to ground

I_p is the source current injected into the bus

In order to handle load flow analysis more conveniently, the use of I_p rather than I_p^* is encouraged. As a result the complex conjugate of the above equation is considered, that is:

$$S_p^* = P_P - jQ_P = V_p^* I_p \tag{3.2}$$

The source current is given by:

$$I_p = \sum Y_{pq} I_{pq} \qquad p = q = 1, 2, 3, ...n \tag{3.3}$$

Thus substituting equation (3.3) in to equation (3.2), we have:

$$P_p - jQ_p = V_p^* \sum Y_{pq} V_q \tag{3.4}$$

The active and reactive power of bus p calculated by equating real and imaginary parts of equation (3.4) above:

$$P_P = Re(V_p^* \sum Y_{pq} V_q) \tag{3.5}$$

$$Q_P = Re(V_p^* \sum Y_{pq} V_q) \tag{3.6}$$

The voltage and bus admittance of the power system can be expressed in polar form as:

$$V_P = |V_P| e^{j\delta_p} \tag{3.7}$$

$$Y_{pq} = |Y_{pq}| e^{j\theta_{pq}} \tag{3.8}$$

where;

θ_{pq} is the angle of the pq^{th} element of the Y_{bus} matrix

Substituting the polar representations given in the equation (3.7) and (3.8) above into equation (3.5) and (3.6), the real and reactive powers expressed in general as shown:

$$P_P = |V_P| \sum |V_q||Y_{pq}| cos(\theta_{pq} + \delta_{pq}) \qquad p = q = 1, 2, \ldots, n \tag{3.9}$$

$$Q_P = -|V_P| \sum |V_q||Y_{pq}| sin(\theta_{pq} + \delta_{pq}) \qquad p = q = 1, 2, \ldots., n \tag{3.10}$$

3.2.1 Analysis of Change in Active Power Flow

The active power flow in a line k connecting two buses, bus p and bus q can be expressed as:

$$P_{pq} = V_P V_q Y_{pq} cos(\theta_{pq} + \delta_{pq}) - V_p^2 Y_{pq} cos\theta_{pq} \tag{3.11}$$

Where;

V_P and V_q are the voltage magnitudes at buses p and q respectively

δ_p and δ_q are the voltage angles at buses p and q respectively

Y_{pq} is magnitude of the pq^{th}element of the Y_{bus} matrix

θ_{pq} is the angle of the pq^{th} element of the Y_{bus} matrix

Mathematically, the active power flow sensitivity can be expressed as:

$$\begin{bmatrix} \frac{\Delta P_{pq}}{\Delta P_n} \\ \frac{\Delta P_{pq}}{\Delta Q_n} \end{bmatrix} \tag{3.12}$$

Ignoring second and higher order terms the change in real line flow using Taylor series approximation can be expressed as:

$$\Delta P_{pq} = \frac{\partial P_{pq}}{\partial \delta_p}\Delta\delta_p + \frac{\partial P_{pq}}{\partial \delta_q}\Delta\delta_q + \frac{\partial P_{pq}}{\partial V_p}\Delta V_p + \frac{\partial P_{pq}}{\partial V_q}\Delta V_q \tag{3.13}$$

The partial derivatives of real power flow with respect to variables δ and V gives the coefficients appearing in the equation (3.13) above as shown below:

$$\frac{\partial P_{pq}}{\partial \delta_p} = V_P V_q Y_{pq} \sin(\theta_{pq} + \delta_{pq}) \tag{3.14}$$

$$\frac{\partial P_{pq}}{\partial \delta_q} = -V_P V_q Y_{pq} \sin(\theta_{pq} + \delta_{pq}) \tag{3.15}$$

$$\frac{\partial P_{pq}}{\partial V_p} = V_q Y_{pq} \cos(\theta_{pq} + \delta_{pq}) - 2V_p Y_{pq} \cos\theta_{pq} \tag{3.16}$$

$$\frac{\partial P_{pq}}{\partial V_q} = V_p Y_{pq} \cos\theta_{pq} \tag{3.17}$$

3.2.2 Analysis of Change in Reactive Power Flow

The reactive power flow in a line k connecting two buses, bus p and bus q can be expressed as:

$$Q_{pq} = -V_P V_q Y_{pq} sin(\theta_{pq} + \delta_{pq}) + V_p^2 Y_{pq} sin\theta_{pq} \tag{3.18}$$

Mathematically, the reactive power flow sensitivity can be written as:

$$\begin{bmatrix} \frac{\Delta Q_{pq}}{\Delta P_n} \\ \frac{\Delta Q_{pq}}{\Delta Q_n} \end{bmatrix} \tag{3.19}$$

Ignoring second and higher order terms the change in reactive line flow using Taylor series approximation can be expressed as:

$$\Delta Q_{pq} = \frac{\partial Q_{pq}}{\partial \delta_p}\Delta\delta_p + \frac{\partial Q_{pq}}{\partial \delta_q}\Delta\delta_q + \frac{\partial Q_{pq}}{\partial V_p}\Delta V_p + \frac{\partial Q_{pq}}{\partial V_q}\Delta V_q \tag{3.20}$$

The coefficients appearing in the equation (3.20) can be obtained using the partial derivatives of real power flow with respect to variables δ and V as shown below:

$$\frac{\partial Q_{pq}}{\partial \delta_p} = V_P V_q Y_{pq}\cos(\theta_{pq} + \delta_{pq}) \tag{3.21}$$

$$\frac{\partial Q_{pq}}{\partial \delta_q} = -V_P V_q Y_{pq}\cos(\theta_{pq} + \delta_{pq}) \tag{3.22}$$

$$\frac{\partial Q_{pq}}{\partial V_p} = -V_q Y_{pq}\sin(\theta_{pq} + \delta_{pq}) + V_p Y_{pq}\cos\theta_{pq} \tag{3.23}$$

$$\frac{\partial Q_{pq}}{\partial V q} = -V_p Y_{pq}\sin(\theta_{pq} + \delta_{pq}) \tag{3.24}$$

3.2.3 Formulating the Sensitivity Factors for Power Flow

The change in the real power flow over a transmission or distribution line connected between bus-p and bus-q due to the change in active power injected at any other bus represents sensitivity factors for the real power flow. Similarly, the change in the reactive power flow over a transmission or distribution line connected between bus p and bus q due to the change in reactive power injected at any other bus represents sensitivity factors for the reactive power flow. The equations for the changes in the line flows arranged in matrix form and expressed as:

$$\begin{bmatrix} \Delta P_{pq} \\ \Delta Q_{pq} \end{bmatrix} = \begin{bmatrix} \frac{\partial P_{pq}}{\partial \delta} & \frac{\partial P_{pq}}{\partial V} \\ \frac{\partial Q_{pq}}{\partial \delta} & \frac{\partial Q_{pq}}{\partial V} \end{bmatrix} \begin{bmatrix} \Delta\delta \\ \Delta V \end{bmatrix} \tag{3.25}$$

The variables $\Delta\delta$ and ΔV can be obtained from the full Newton Raphson load flow Jacobian matrix as follows:

$$\begin{bmatrix} \Delta P \\ \Delta Q \end{bmatrix} = [J] \begin{bmatrix} \Delta\delta \\ \Delta V \end{bmatrix} = \begin{bmatrix} J_1 & J_2 \\ J_3 & J_4 \end{bmatrix} \begin{bmatrix} \Delta\delta \\ \Delta V \end{bmatrix} \tag{3.26}$$

Then the variables $\Delta\delta$ and ΔV can be obtained from equation (3.26)above as:

$$\begin{bmatrix} \Delta\delta \\ \Delta V \end{bmatrix} = \begin{bmatrix} J_1 & J_2 \\ J_3 & J_4 \end{bmatrix}^{-1} \begin{bmatrix} \Delta P \\ \Delta Q \end{bmatrix} \tag{3.27}$$

Now substituting equation (3.27) for $\Delta\delta$ and ΔV into equation (3.25) for the change in line flows we have:

$$\begin{bmatrix} \Delta P_{pq} \\ \Delta Q_{pq} \end{bmatrix} = \begin{bmatrix} \frac{\partial P_{pq}}{\partial \delta} & \frac{\partial P_{pq}}{\partial V} \\ \frac{\partial Q_{pq}}{\partial \delta} & \frac{\partial Q_{pq}}{\partial V} \end{bmatrix} \begin{bmatrix} J_1 & J_2 \\ J_3 & J_4 \end{bmatrix}^{-1} \begin{bmatrix} \Delta P \\ \Delta Q \end{bmatrix} \tag{3.28}$$

The sensitivity factors for the real power flows are represented as:

$$\begin{bmatrix} \frac{\partial P_{pq}}{\partial P_n} \\ \frac{\partial P_{pq}}{\partial Q_n} \end{bmatrix} = \begin{bmatrix} L_{PP} \\ L_{PQ} \end{bmatrix} = \left[J^T\right]^{-1} \begin{bmatrix} \frac{\partial P_{pq}}{\partial \delta} \\ \frac{\partial P_{pq}}{\partial V} \end{bmatrix} \tag{3.29}$$

The sensitivity factors for the reactive power flows are represented as;

$$\begin{bmatrix} \frac{\partial Q_{pq}}{\partial P_n} \\ \frac{\partial Q_{pq}}{\partial Q_n} \end{bmatrix} = \begin{bmatrix} L_{QP} \\ L_{QQ} \end{bmatrix} = \left[J^T\right]^{-1} \begin{bmatrix} \frac{\partial Q_{pq}}{\partial \delta} \\ \frac{\partial Q_{pq}}{\partial V} \end{bmatrix} \tag{3.30}$$

Where;

L_{PP} is the real power flow sensitivity related to the real power injection

L_{PQ} is the active flow sensitivity related to the reactive power injection

L_{QP} is the reactive power flow sensitivity related to the active power injection

L_{QQ} is the reactive power flow sensitivity related to the reactive power injection

J is the Jacobian matrix of power flow, and the superscript T indicates the transpose

Here the four sensitivities are column vectors with dimension of the number of the system busses.

3.2.4 Analysis of Change in Real Power Loss

The real power loss in a line connecting two buses, bus p and bus q can be expressed as:

$$P_{L(pq)} = \alpha_{pq}\left({V_p}^2 + {V_q}^2 - 2V_pV_q\cos(\delta_{pq})\right) \tag{3.31}$$

Thus, the total active power loss in the circuit can be expressed as:

$$P_{L(total)} = \sum_{i=1}^{nb} \left[\alpha_{pq} \left({V_p}^2 + {V_q}^2 - 2V_pV_q \cos(\delta_{pq})\right)\right] \tag{3.32}$$

Where;

nb is the number of lines of the network

α_{pq} is the conductance of the line $p-q$

V_p is the nodal voltage of bus p

V_q is the nodal voltage of bus q

δ_{pq} is the phase angle difference between the busses p and q

Mathematically, loss sensitivity for the real power can be written as:

$$\begin{bmatrix} \frac{\Delta P_{L(pq)}}{\Delta P_n} \\ \frac{\Delta P_{L(pq)}}{\Delta Q_n} \end{bmatrix} \tag{3.33}$$

Ignoring second and higher order terms the change in real power loss using Taylor series approximation can be expressed as:

$$\Delta P_{L(pq)} = \frac{\partial P_{L(pq)}}{\partial \delta_p}\Delta\delta_p + \frac{\partial P_{L(pq)}}{\partial \delta_q}\Delta\delta_q + \frac{\partial P_{L(pq)}}{\partial V_p}\Delta V_p + \frac{\partial P_{L(pq)}}{\partial V_q}\Delta V_q \tag{3.34}$$

The partial derivatives of real power loss with respect to variables δ and V gives the coefficients appearing in the equation (3.34) above as shown below:

$$\frac{\Delta P_{L(pq)}}{\partial \delta_p} = 2\alpha_{pq}V_pV_q \sin(\delta_{pq}) \tag{3.35}$$

$$\frac{\Delta P_{L(pq)}}{\partial \delta_q} = -2\alpha_{pq}V_pV_q \sin(\delta_{pq}) \tag{3.36}$$

$$\frac{\Delta P_{L(pq)}}{\partial V_p} = 2\alpha_{pq}(V_p - V_q \sin\delta_{pq}) \tag{3.37}$$

$$\frac{\Delta P_{L(pq)}}{\partial V_q} = 2\alpha_{pq}(V_q - V_p \sin\delta_{pq}) \tag{3.38}$$

3.2.5 Analysis of change in Reactive Power Loss

The reactive power loss in a line connecting two buses, bus p and bus q can be expressed as:

$$Q_{L(total)} = \sum_{i=1}^{nb} \left[-{b_{pq}}^{sh}({V_p}^2 + {V_q}^2) - b_{pq}({V_p}^2 + {V_q}^2 - 2V_pV_q \cos\delta_{pq})\right] \tag{3.39}$$

Where;

b_{pq}^{sh} is the shunt susceptance of the line p-q

b_{pq} is the susceptance of the line p-q

Mathematically, loss sensitivity for the reactive power can be written as:

$$\begin{bmatrix} \frac{\Delta Q_{L(pq)}}{\Delta P_n} \\ \frac{\Delta Q_{L(pq)}}{\Delta Q_n} \end{bmatrix} \tag{3.40}$$

Ignoring second and higher order terms the change in reactive power loss using Taylor series approximation can be expressed as:

$$\Delta Q_{L(pq)} = \frac{\partial Q_{L(pq)}}{\partial \delta_p}\Delta\delta_p + \frac{\partial Q_{L(pq)}}{\partial \delta_q}\Delta\delta_q + \frac{\partial Q_{L(pq)}}{\partial V_p}\Delta V_p + \frac{\partial Q_{L(pq)}}{\partial V_q}\Delta V_q \tag{3.41}$$

The partial derivatives of reactive power loss with respect to variables δ and V gives the coefficients appearing in the equation (3.41) above as shown below:

$$\frac{\Delta Q_{L(pq)}}{\partial \delta_p} = 2b_{pq}V_pV_q\sin(\delta_{pq}) \tag{3.42}$$

$$\frac{\Delta Q_{L(pq)}}{\partial \delta_q} = -2b_{pq}V_pV_q\sin(\delta_{pq}) \tag{3.43}$$

$$\frac{\Delta Q_{L(pq)}}{\partial V_p} = -2[{b_{pq}}^{sh}V_p + b_{pq}(V_p - V_q\cos(\delta_{pq})) \tag{3.44}$$

$$\frac{\Delta Q_{L(pq)}}{\partial V_q} = -2[{b_{pq}}^{sh}V_q + b_{pq}(V_q - V_p\cos(\delta_{pq})) \tag{3.45}$$

3.2.6 The Power Loss Sensitivity Factors Formulation

The change in the real power loss over a transmission or distribution line connected between bus-p and bus-q due to the change in active power injected at any other bus represents the sensitivity factors for real power loss. Similarly, the change in the reactive power loss over a transmission or distribution line connected between bus-p and bus-q due to the change in reactive power injected at any other bus represents sensitivity factors for reactive power loss. To calculate the changes in the line flows the equations can be arranged in matrix form as:

$$\begin{bmatrix} \Delta P_{L(pq)} \\ \Delta Q_{L(pq)} \end{bmatrix} = \begin{bmatrix} \frac{\partial P_{L(pq)}}{\partial \delta} & \frac{\partial P_{L(pq)}}{\partial V} \\ \frac{\partial Q_{L(pq)}}{\partial \delta} & \frac{\partial Q_{L(pq)}}{\partial V} \end{bmatrix} \begin{bmatrix} \Delta\delta \\ \Delta V \end{bmatrix} \tag{3.46}$$

Applying the same procedure similar to the sensitivity factors for the real and reactive power flows, the sensitivity factors for the real and reactive power loss represented by:

$$\begin{bmatrix} \frac{\partial P_{L(pq)}}{\partial P_n} \\ \frac{\partial P_{L(pq)}}{\partial Q_n} \end{bmatrix} = \begin{bmatrix} M_{PP} \\ M_{PQ} \end{bmatrix} = \left[J^T\right]^{-1} \begin{bmatrix} \frac{\partial P_{L(pq)}}{\partial \delta} \\ \frac{\partial P_{L(pq)}}{\partial V} \end{bmatrix} \tag{3.47}$$

$$\begin{bmatrix} \frac{\partial Q_{L(pq)}}{\partial P_n} \\ \frac{\partial Q_{L(pq)}}{\partial Q_n} \end{bmatrix} = \begin{bmatrix} M_{QP} \\ M_{QQ} \end{bmatrix} = \left[J^T\right]^{-1} \begin{bmatrix} \frac{\partial Q_{L(pq)}}{\partial \delta} \\ \frac{\partial Q_{L(pq)}}{\partial V} \end{bmatrix} \tag{3.48}$$

Where;

M_{PP} is the real power loss sensitivity related to the real power injection

M_{PQ} is the real power loss sensitivity related to the reactive power injection

M_{QP} is the reactive power loss sensitivity related to the active power injection

M_{QQ} is the reactive power loss sensitivity related to the reactive power injection

Here the four sensitivities are column vectors with dimension of number of the system busses.

3.3 Objective Function Formulation

Integrating DG in the distribution system is mainly to minimize power losses, voltage drop and to maximize the stability and reliability of the power distribution system. In this paper, the proposed multi-objective Harish hawks optimization method aims to minimize the power loss, voltage deviation, and total operating cost of the distribution system. The performance index is computed for each objective function to optimally locate and sizing of DG units and to enhance the voltage stability of the radial distribution system. Mathematically, the expression for objective functions and constraints are formulated in the following subsection.

3.3.1 Minimizing Real Power Losses

The radial structure of the power system increase active power losses in the distribution system hence, it is important to reduce the active power losses (PL).

$$Min, PL = \sum\nolimits_{i=1}^{nb} (\mathrm{I_i}^2 \times R_\mathrm{i}) \tag{3.49}$$

Where;

i is the branch number

N_b is the total number of branches

R_i is branch resistance

3.3.2 Minimizing Reactive Power Losses

Most papers do not consider reactive power loss minimization as the objective function.In this thesis,the reactive power loss (QL) also included along with real power loss for calculating optimal DG sizes and location.

$$Min, QL = \sum_{i=1}^{nb} (\mathrm{I_i}^2 \times X_\mathrm{i}) \tag{3.50}$$

Where;

X_i is branch reactance

3.3.3 Minimizing Voltage Drop

By installing the DG, the proposed method will try to minimize the voltage drop(VD) by minimizing the gap between the rated voltage that is usually one and the actual voltage of the bus nearer to zero. Therefore, it improves the voltage stability and the network performance.

$$Min, VD = \sum_{i=1}^{Nn} (\mathrm{V_{ni}} - V_{\mathrm{rated}})^2 \tag{3.51}$$

Where;

Nn is total number of bus

N_i is receiving bus number

V_{ni} is voltage of bus Ni

V_{rated} is the rated voltage

3.3.4 Minimizing Annual Economic Loss

The problem is finding the best combination of some DG units among available categories and placing them on suitable buses not only to minimize the power loss but also to

minimize the annual cost of losses and installed units. It is not advisable to install a very high-capacity DG in the network as it increase the cost of real power supplied by the DG. Here the system has two operational costs one from the real power supplied from the substation and the other from real power drawn from the DG. The cost from the substation can be minimized by reducing the total loss of the system and the cost of the DG can be minimized by reducing the size of the DG. After integrating DGs in to the network, the total active power loss with DG (PL_{WDG}) is reduced compared to total active power loss without DG (PL_{WODG}). Therefore, total Annual Economic Loss without any DG (AEC_{WODG}) given by the equation below:

$$\mathrm{AEC_{WODG}} = \mathrm{PL_{WODG}} \times C_e \times 8760 \tag{3.52}$$

Where; C_e = Energy loss cost per kWh in birr

Total Annually Economic Loss with DGs (AEC_{WDG}) will be:

$$\mathrm{AEC_{WDG}} = \mathrm{PL_{WDG}} \times C_e \times 8760 + \frac{C_{DG} \sum_{i=1}^{N_{DG}} P_{DG}}{L_T} \tag{3.53}$$

Where;

N_{DG} is Number of DG installed in the system

C_{DG} is Cost of DG generated power per kW

L_T is Total DG life in years

So, Annual Savings(AS) is calculated as:

$$\mathrm{AS} = \mathrm{AEC_{WODG}} - \mathrm{AEC_{WDG}} \tag{3.54}$$

3.4 Objective Function Index

To evaluate the performance of the system at each objective function the performance index namely real power loss reduction index, reactive power loss reduction index, voltage profile improvement, and annual economic loss reduction index are takes into consideration in the objective function.

3.4.1 Real Power Loss Reduction Index

A common strategy for sizing and placement of DG is to minimize system power loss of the power system. The total active power loss reduction index (PLRI) is the ratio of percentage reduction in real power loss from the base case when a DG is installed which is expressed in the equation as below:

$$\text{PLRI} = \frac{PL_{\text{WDG}}}{PL_{\text{WODG}}} \tag{3.55}$$

Where;

PL_{WODG} is the total active power loss before DG installation

PL_{WDG} is the total active power loss in the system after installation of DG

By minimizing (PLRI), the reduction in real power losses in the presence of DGs unit will be a maximum value.

3.4.2 Reactive Power Loss Reduction Index

To determine the effect of DG on reactive power losses, the Reactive Power Loss Reduction Index is incorporated as an objective function. This refers to the ratio of percentage reduction in reactive power loss from base case when a DG is installed at bus i.

Reactive Power Loss Reduction Index (QLRI) is expressed as:

$$\text{QLRI} = \frac{QL_{\text{WDG}}}{QL_{\text{WODG}}} \tag{3.56}$$

Where;

QL_{WODG} is the total reactive power loss before DG installation

QL_{WDG} is the total reactive power loss in the system after installation of DG

3.4.3 Voltage Deviation Index

In a power system, the voltage at each bus should be within the acceptable range and the line flow within the limits. These limits are important so that the integration of distributed generation into the system does not increase the cost for voltage control or replacement of existing lines.

The Voltage Deviation Index (VDI) help to identify the size-location pair, which gives higher voltage improvement from the base voltage and is defined as:

$$VDI = \frac{VD_{\text{WDG}}}{VD_{\text{WODG}}} \tag{3.57}$$

Where;

VD_{WODG} is total voltage drop without DG

VD_{WDG} is total voltage drop with DG

3.4.4 Annual Cost Reduction Index

This refers to the ratio of percentage reduction in annual operating cost from base case when a DG is installed at a selected bus. The Annual cost of reduction Index (ACRI) defined as follow:

$$\text{ACRI} = \frac{AEC_{\text{WDG}}}{AEC_{\text{WODG}}} \tag{3.58}$$

3.5 Multi-objective Function Formulation

The separate objective functions index listed above combined together to form the multi-objective function of the distribution networks using the weighting factor. The MOF is a multiple index function proposed to be optimal location and sizing of DG units and to enhance the optimal operation of the radial distribution system. The lowest values of PLRI, QLRI, and VDI are to reduce the real, reactive power losses and voltage drop of the distribution system respectively. The multi-objective function (MOF) formulated in the equation below as:

$$MOF = W_1 + W_2 + W_3 + W_4 \tag{3.59}$$

The values of weighting factors play an important role in optimizing the multi-objective problem, and are decided according to the network designer at which it optimize the system. The values of the weighting factors will be larger weight for the individual objective function that outperforms the others higher in terms of importance and benefits and vice versa. The sum of the weight factors assigned to all individual objective function should add up to one. That is:

$$W_1 + W_2 + W_3 + W_4 = 1 \tag{3.60}$$

3.6 Constraints Formulation

The aim is to minimize the multi-objective function formulated above subjected to various inequality and equality operational constraints so as satisfy to the electrical requirements for the distribution network.

3.6.1 Real and Reactive Power balance constraints

Power balance is similar to the non-linear power flow equations, which state that the sum of complex power flows at each bus in the distribution system injected into a bus minus the power flows extracted from the bus including line losses should equal zero. The constraints for power balance formulated as follows:

$$P_i = P_{DGi} - (P_{Di} - P_{Li}) \tag{3.61}$$

$$Q_i = Q_{DGi} - (Q_{Di} - Q_{Li}) \tag{3.62}$$

Where;

P_i is real power flow at bus i in KW

Q_i is reactive power flow at bus i in KVAr

P_{DGi} is distributed real power generations at bus i in KW

Q_{DGi} is distributed real power generations at bus i in KW

P_{Di} is real power demand at bus i in KW

Q_{Di} is reactive power demand at bus i in KVAr

P_{Li} is real power loss at bus i in KW

Q_{Li} is reactive power loss at bus i in KVAr

3.6.2 Bus Voltage Limits

This includes the upper and lower voltage magnitude limit, V_{min} and V_{max} at each node. Bus Voltage magnitude is to be within acceptable operating limits throughout the optimization process to maintain power quality and failure of electrical device.

The bus voltage limit of the system given by:

$$V_{\min} \leq V_i \leq V_{\max} \tag{3.63}$$

Where;

V_{min} and V_{max} are lower and upper bound of bus voltage limits in p. u

3.6.3 DG Capacities

The DG capacity of each unit should be defined around its nominal value to operate the system within the acceptable limit. So that each DG unit is maintained within an acceptable limit. This includes the upper and lower real and reactive power generation limits of distributed generators (DGs) connected at each bus. The capacity of DG is given as follows:

$$PDG_{\min} \leq PDG_i \leq PDG_{\max} \tag{3.64}$$

$$QDG_{\min} \leq QDG_i \leq QDG_{\max} \tag{3.65}$$

Where;

PDG_{min} is the minimum real power generation from DG capacity in KW

PDG_{max} is the maximum real power generation from DG capacity in KW

QDG_{min} is the minimum reactive power generation from DG capacity in KVAr

QDG_{max} is the maximum reactive power generation from DG capacity in KVAr

3.7 Optimization Techniques

Up to now, many intelligent search techniques have been proposed and developed to solve the optimization problems that are complex problems instead of using traditional methods due to their accuracy and robustness. In this paper, three different algorithms having different decision-making process are explained below and HHO is selected as it is effective compared to them in searching the optimal point.

3.7.1 Genetic Algorithm

There are many optimization algorithm techniques for solving optimization problems. Due to the limitation of classical optimization methods in finding global minimum value, the heuristic optimization methods are widely used because of their reliability, flexibility, and robustness in seeking optimum value in recent years [42]. GA is a heuristic search method to find the global optimal solution in a complex multi-dimensional search space.

The Genetic Algorithm is used to solve an optimization problem with objective function based on the mechanism of the natural selection and evolution that is survival of the fittest. To find the best fitness, GA needs the initial value and randomly generates individual solutions. The objective function used to calculate the fitness of each randomly generated individual population to select the most fitted individuals and let them generate more fit individuals, just like evolution in nature.

More generations are produced by applying GA operators. This eventually leads to a generation of high performing individuals. A typical genetic algorithm mainly finds the optimal point usually based on three operators [43]: production operator (elitism), recombination (also known as the crossover) operator, and mutation operator. GA needs to combine to a method that has good convergence such as PSO to obtain a robust solution for the problem at hand.

3.7.1.1 Choice of GA Parameters

GA parameters are crucial for its faster convergence, depend on its selection. In the absence of any guiding rule to choose these parameters, some mechanism has to be developed. The GA parameters include:

Population size

Initially, the genetic algorithm creates many chromosomes randomly under the constraint conditions. The number of chromosomes named as a possible solution to the problems is the population size. Enlarging the population size leads to more accurate solutions increasing the search scope. However, it is not always necessary to have so large population. Therefore, the researchers should find a suitable size of population. This initial population is a set of many possible solutions evaluated on the main goal of the problem to see if it is a good or bad answer. The genetic algorithm will start from this generation, and select and inherit the high fitness individuals for the next generation.

The best solutions compared to each other until we reach the stopping criteria to find the best answer.

Selection

The chromosomes of the population sorted based on their fitness value and selecting individuals with high fitness and grouping these individuals into a new population according to the fitness value to keep the better individuals for the next generation, thereby making the individuals in the population come close to the optimal solution gradually. The chromosomes mixed to other chromosomes with less fitness to generate the next population (or change the current population intelligently). The chromosomes with a higher amount of fitness copied than others even if each chromosome has its own probability. Generally, the selection process determines the number of solution to be selected from the current population to create the new generation, and which of the current solutions should be erased to make room for new solutions. The most commonly used scheme for the process of selection is Roulette Wheel Selection. The roulette wheel operates based on the fitness of each of the solution candidates.

Crossover

In genetic algorithms, the purpose of the crossover operator is to randomize recombination operations and to change the programming of chromosomes by exchange genetic information between two selected solutions from the current population (parents) that produces unique new solutions to be included in the next generation. It is also a recombination process of taking more than one parent solution and producing a child solution from them. Generally, the types of crossover are one-point, two-point, and N-point, and random multipoint crossover and the choice of mutation depends on the user. The underlying idea in the crossover operation is that "good" solutions may produce better ones by interchanging their genetic material. A crossover operator is typically applied to a percentage of selected solutions determined by the parameter called the crossover probability (Pc). Typical values for Pc are in the range of 0.6-0.9 [44].

Mutation

Mutation removes the overcome in the crossover by creating new genetic material in the population to maintain diversity transformation of gene from one generation of a population of genetic algorithm chromosomes to the next. It used to changes the new solution completely from the old result by changing one or more gene values in a chromosome from

its initial state. The rate of its occurrence determined by the parameter called the probability of mutation, Pm, with typical values in the range of 0-1 [45]. GA follows different types of mutation like bit string mutation, flip bit mutation, uniform and non-uniform mutation to implement the process.

Elitism

Elitism is the genetic operator implemented to put the most fit individuals in the next generation and to replace the worst chromosome in the newly generated population with the best chromosome in the old population. This is operated if the best number in the newly generated population is worse than that in the old population and to ensure the algorithm's convergence. It used to preserve the elite parent.

3.7.2 Particle Swarm Optimization

Particle swarm optimization (PSO) is a metaheuristic algorithm based on the concept of swarm intelligence. PSO proposed by Eberhart and Kennedy in 1995, considering social behavior in the flocks of birds that flew together [46]. It takes its operation based on the movement of organisms and social behavior of animals such as birds, fishes, insects, their communities, and the members of the entire population maintained through the search procedure. PSO focused on how they manage as a group, rather than as individuals, recreating themselves and adapting in accordance with the changes in the surrounding environment, to search for food or to migrate.

It was imitated the behavior of individual swarms which are a flock of birds, school of fish, and other insect groups and optimizes a problem by improving, in an iterative way, candidate solutions called particles regarding a given measure of quality.

In a PSO algorithm, the particle is an individual member & each particle flies around the multi-dimensional search space with a velocity and position. The particle updates its velocity and position continuously comparing itself with its own experience and experience of the neighbor's particles or the experience of the whole swarm. Then each particle moved through the information related to best personal position (Pbest) and best global position (Gbest). The mathematical expression of the algorithm also expressed in the following

equations.

$$V_i^{(k+1)} = V_i^k + c_1 * r_1(X_{\text{Pbest}} - \text{X}_i^k) + c_2 * r_2(X_{\text{Gbest}} - \text{X}_i^k) \tag{3.66}$$

$$X_i^{(k+1)} = X_i^k + V_i^{(k+1)} \tag{3.67}$$

Where;

X_i^k is the current individual position of particle i at iteration k

X_i^{k+1} is modified position of particle i

V_i^k is the velocity of particle i of the previous vector at iteration k

V_i^{k+1} is modified velocity of particle i

c_1, c_2 are random number between [0 1]

X_{Pbest} is the personal best position of a particle

X_{Gbest} is the global best position of the particle

3.7.3 Proposed Harris Hawks Optimization (HHO) Algorithm

Harris Hawks Optimizer (HHO) is a new novel population-based, nature-inspired optimization based on the cooperative hunting behavior of the most intelligent and distinguished predator birds in nature. In this intelligent strategy, several hawks from different directions cooperatively pounce the potential animal (rabbit) in a group for its food. Initially, a group of hawks is considered as the initial population that tries to chase the targeted prey rabbit from different directions, and initially, the leader hawk tries to attack the prey [47]. If the leader hawks fail to grab the prey because of the dynamic nature and escaping behavior of the prey, the switching tactics are followed, so that the other party members (hawks in the group) will hit the escaped prey until seized.

HHO is applied for determining the optimal size and location of DG at different operating power factors (pf) with the aim of minimizing the total active power loss, reducing the voltage deviation (VD), and increasing the voltage stability (VS) considering the operational constraints of the distribution system. It is effective for any optimization problem subject to a proper formulation using exploration and exploitation phases and its performance is improved using the rabbit location instead of the random location. The mathematical formulation of each phase of the proposed HHO inspired by exploring a prey, surprise pounce, and different attacking strategies of Harris hawks presented in the

following subsections:

3.7.3.1 Exploration phase

The exploration phase based on the concept of a group of hawks try to perch randomly on some locations and wait to detect a prey. The group of hawks can track and detect the prey usually a rabbit by their powerful eyes. The leader hawks perch based on the position of family members and prey to detect a prey maybe after several hours since the position of prey cannot see easily.

The exploration process in HHO can be expressed using two strategies. Firstly, when the hawks and family member locations close enough for the condition of $q < 0.5$ and the second strategy is when the hawks located at random trees for condition of $q \geq 0.5$. The mathematical implementation of these strategies is modeled as:

$$X(t+1) = \begin{cases} X_{\text{rand}}(t) - r_1 |X_{\text{rand}}(t) - 2r_2 X(t)| & q \geq 0.5 \\ (X_{\text{rabbit}}(t) - X_m(t)) - r_3(LB + r_4(UB - LB)) & q < 0.5 \end{cases} \tag{3.68}$$

Where;

t is the current iteration

$X(t+1)$ is the position vector of hawks in the next iteration

$X_{rand}(t)$ is a randomly selected hawk from the current population

$X_{rabbit}(t)$ is the position of rabbit

$X(t)$ is the current position vector of hawks

r_1, r_2, r_3, r_4, and q are random numbers between (0, 1), which are updated in each iteration

LB and UB show the upper and lower bounds of variables

X_m is the average position of the current population of hawks

The average position of the current population of hawks mathematically expressed as:

$$X_m(t) = \frac{1}{N} \sum_{i=1}^{N} X_i(t) \tag{3.69}$$

Where;

X_i(t) indicates the location of each hawk at iteration t

N denotes the total number of hawks

3.7.3.2 Transition from exploration to exploitation

The value of the escaping energy (E) of the prey determines the transition from exploration to exploitation phase and different exploitative behaviors. The energy of a prey usually the rabbit decreases considerably during the chasing or escaping behavior. The energy of a prey mathematically modeled as:

$$E = 2E_O(1 - \frac{t}{T}) \tag{3.70}$$

Where;

E indicates the escaping energy of the prey

T is the maximum number of iterations

E_o is the initial state of its energy changes randomly between -1 and 1

When the value of E_o decreases from 0 to -1, it indicates that the rabbit is physically flagging and when the value of E_o increases from 0 to 1, the rabbit is strengthening. During the iterations, the initial state of energy E_o have a decreasing or increasing trend while the dynamic escaping energy E has a decreasing trend. The HHO performs the exploration phase when the escaping energy $|E| \geq 1$, hence, the hawks search different regions to explore a rabbit location, and HHO starts exploiting near to the rabbit place when $|E| < 1$.

3.7.3.3 Exploitation phase

In the HHO, the chance of the rabbit to escape (r) and escaping energy (E) determine whether the exploitation phase implemented or not. In this phase, the Harris' hawks perform the switching tactics to attack the intended prey based on the escaping behaviors of the prey and the chasing strategies of the Harris' hawks. The exploitation phase performed in four possible strategies to model the attacking stage. When $r < 0.5$, the chance of a prey named as successfully escaping and not when $r \geq 0.5$ before surprise pounce.

The hawks increase the probability of killing the rabbit by attacking the prey from different directions named as a hard or soft besiege. After several minutes, the escaping prey will lose its energy and the hawks get closer to the intended prey to intensify the besiege process and effortlessly catch the exhausted prey.

The HHO optimization utilizes the escaping energy E to switch between soft and hard besiege processes. In this regard, when $r \geq 0.5$ and $|E| \geq 0.5$, the soft besiege happens, and when $r \geq 0.5$ and $|E| < 0.5$, the hard besiege occurs.

3.7.3.4 Soft besiege

During soft besiege, the rabbit has enough energy and tries to escape with the aid of random jumps notwithstanding the hawks surround it softly. The soft besiege performed when both of the chance of the rabbit to escape (r) and absolute value of the escaping energy $(E) \geq 0.5$. During these attempts, the Harris' hawks encircle it softly to make the rabbit more exhausted and then perform the surprise pounce. Mathematically this besiege modeled as follow:

$$X(t+1) = \Delta X(t) - E|JX_{\text{rabbit}}(t) - X(t)| \tag{3.71}$$

$$J = 2(1 - r_5) \tag{3.72}$$

$$\Delta X(t) = X_{\text{rabbit}}(t) - X(t) \tag{3.73}$$

Where;

$\Delta X(t)$ is the difference between the position vector of the rabbit and the current location in iteration t

r_5 is a random number inside (0, 1)

J represents the random jump strength of the rabbit throughout the escaping procedure

3.7.3.5 Hard besiege

The hard besiege performed when $r \geq 0.5$ and $|E| < 0.5$, the prey is so exhausted and it has a low escaping energy while the hawks hardly surrounded the intended prey to finally perform the surprise pounce. In this situation, the action mathematically formulated as:

$$X(t+1) = X_{\text{rabbit}}(t) - E|\Delta X(t)| \tag{3.74}$$

3.7.3.6 Soft besiege with progressive rapid dives

This besiege performed when $r < 0.5$ and $|E| \geq 0.5$ in which the rabbit has enough energy to successfully escape and still a soft besiege is constructed before the surprise

pounce. The main besiege that distinguishes the HHO over the other swarm methods is soft besiege with progressive rapid dives, which is an intelligence strategy than the previous case. This besiege is mathematically formulated based on the concept of the levy flight (LF), the escaping patterns of the prey, and leapfrog movements as follow:

$$Y = X_{\text{rabbit}}(t) - E|JX_{\text{rabbit}}(t) - X(t)| \tag{3.75}$$

Where;

Y denotes the soft besiege position

The hawks dive based on the LF-based patterns using the following equation:

$$Z = Y + S \times LF(D) \tag{3.76}$$

Where;

D indicates the problem dimension

S is a vector of random values with dimension $1 \times D$

The levy flight (LF) mathematically expressed as:

$$LF(x) = 0.01 \times \frac{w \times \delta}{u^{\frac{1}{\beta}}} \tag{3.77}$$

$$\delta = (\frac{\Gamma(1+\beta \times \sin(\frac{\pi\beta}{2}))}{\Gamma(\frac{(1+\beta)}{2}) \times \beta \times 2^{(\frac{\beta-1}{2})}})\frac{1}{\beta} \tag{3.78}$$

Where;

w and u are random values inside (0,1)

β is a default constant set to 1.5

Hence, the final strategy for updating the positions of hawks in the soft besiege phase can be performed by equation (3.79):

$$X(t+1) = \begin{cases} Y\ if F(Y) < F(X(t)) \\ Z\ if F(Z) < F(X(t)) \end{cases} \tag{3.79}$$

Where;

Y and Z are obtained using equation (3.75) and (3.76)

3.7.3.7 Hard besiege with progressive rapid dives

During this besiege the rabbit has not enough energy to escape and it is performed when $|E| < 0.5$ and $r < 0.5$. The hard besiege is constructed before the surprise pounce to catch and kill the prey. The situation of this step in the prey side is similar to that in the soft besiege, but this time, the hawks try to decrease the distance of their average location with the escaping prey. Therefore, the following rule is performed in hard besiege condition:

$$X(t+1) = \begin{cases} Y\ if F(Y) < F(X(t)) \\ Z\ if F(Z) < F(X(t)) \end{cases} \tag{3.80}$$

Where; Y and Z are obtained using equation bellow as:

$$Y = X_{\text{rabbit}}(t) - E|JX_{\text{rabbit}}(t) - X_m(t)| \tag{3.81}$$

$$Z = Y + S \times LF(D) \tag{3.82}$$

In the proposed HHO algorithm, if the hawks becomes out of the position limits, the following equation is used to restrict the hawks within the minimum and maximum limit of the problem variables:

$$X(t+1) = \begin{cases} X(t+1) & X_{min} \leq X(t+1) \leq X_{max} \\ X_{max} & X(t+1) > X_{max} \\ X_{min} & X(t+1) < X_{max} \end{cases} \tag{3.83}$$

3.7.4 Application of HHO in DG allocation

The application of the HHO into DG allocation can be summarized in the following steps: Where;

Step 1: Read the system data (line and load data) and define the objective function.

Step 2: Randomly initialize a set of hawks' searches within the upper and lower limits of the DG sizes and locations, HHO parameters, and maximum number of iterations K_{max}.

Step 3: Rub the power flow and calculate the objective function for each search hawk.

Step 4: Store the best solution Xrabbit.

Step 5: Update the parameters of HHO (E, E_o, and J).

Step 6: Update the sizes and locations of the best solutions based on the exploration and exploitation phases' strategies.

Step 7: Check the sizes and locations limits and update the position

Step 8: Check if ($k < K_{max}$) Step 2.

Step 9: Return the final best solution stored (DG location and sizes).

Step 10: Run the power flow and obtain the voltage profile.

In this paper, a novel population-based, multi-objective Harris Hawks Optimization algorithms mainly based on the intelligence behavior of the Harris hawks in chasing prey is applied for determining the optimal placement of distribution generation (DG) in the radial distribution systems.

Chapter 4

MODELING OF DFIG BASED WIND ENERGY GENERATION SYSTEM

4.1 Overview of Wind Energy Generation System

The generation and integration of wind power to the grid consists of mechanical and electrical parts like wind turbines, gear, and electrical generators. The size and type of the wind turbine to generate a large amount of energy is determined by the wind speed sources, cut-in and cut-out wind speed mainly to contribute significant renewable fraction and this can be performed using single large wind turbine or number of smaller turbines. The electrical generators mostly used today to convert the wind energy system are either doubly fed induction generator (DFIG) or permanent magnet synchronous generator (PMSG) type. WECS with a Permanent magnet synchronous generator use the synchronous generator to convert the mechanical power from the wind available in the area to electrical power to the grid. PMSG has fewer mechanical stress issues and high efficiency with less maintenance due to the absence of a gearbox [48]. The PMSG is usually a multi-polar generator, which relatively makes the system large and heavy and causes inconvenience for the installation and naturally needs permanent magnets, which will increase the cost for this wind turbine concept considering the current market. The power converters used in PMSG based WTGS are a full-scale power rating, which will cause high losses, generate high harmonic components, and have high cost [49].

WECS with DFIG uses a wound rotor induction electric generator where both windings transfer significant power between shaft and grid. The rotor side windings of the doubly fed induction generator are connected to a back-to-back converter via slip rings, while the stator side windings are directly connected to the grid. The power converters could control the rotor frequency and thus the rotor speed. The power rating of the power converters is typically about 25-30% total generated power since the rotor of the doubly fed induction generator would only deal with slip power and the rest fed to the grid directly from the stator [50]. The smaller rating of the power converters leads to many advantages, such as reduced converter cost, reduced filter volume and cost, less switching losses, less harmonic injections into the connected grid, improved overall efficiency, and reduce overall cost of the system. Besides, this type of wind turbine can also achieve the desired reactive power compensation. The doubly fed induction generator has additional features that allow them to run at a speed slightly above or below their natural synchronous speed which is useful for variable speed wind turbine because wind speed can change suddenly.

Nowadays, the most frequently used wind energy conversion system is using DFIG-based wind turbine-generator system in industry for large wind turbines and a variable speed generator is the preferred option in newer wind turbine installations because of the fact that machine with this technology exhibits more power capture and less mechanical stress [51]. The paper also explains the technology of integrating generator, gearbox, main shaft, and shaft bearing within a common housing, variable speed operation over a large, but restricted, range makes WECS with doubly fed induction generator interesting. This concept makes the system less weight, less size of generators, become cheaper and more reliable system than that of the standard one, but it loses its efficiency.

Considering the merits of the DFIG systems, this thesis will only focus on the modeling and control schemes of DFIG based wind turbine generator systems. Nordex N80/2500 wind turbine taken for this analysis because among the wind turbine available in the market, it start generating power at the lowest cut-in wind speed of 3 m/s. This property is beneficial to low speed regions like those considered in this thesis.The generation of wind energy system requires modeling of wind turbine and generator to integrate the power to the grid.

4.2 Modeling of Wind Turbine system

The modeling of wind turbine systems involves the aerodynamic wind turbine modeling, the drive train system modeling, and the modeling of the wind turbine controller.

4.2.1 Aerodynamic Modeling

There are two arrangement in WECS that converts kinetic energy of air in motion into electrical energy. The first arrangement converts the kinetic energy of the wind flow into the mechanical power to turn the wind turbine rotor. The second one is the generator that transforms the rotational mechanical power to electrical power. The wind speed passing through a turbine rotor plane and the available input power in the wind (P_w) is related in the equation below as:

$$p_w = \frac{1}{2}\rho A V_w^3 \tag{4.1}$$

Where;

ρ is the destiny of air in kg/m^3

A is the swept area measured in m^2

V_w is the available wind speed in m/s

However, the power that can be converted for useful work is limited by a factor called "Betz Limit" which is 0.5925. That means the maximum efficiency that the wind turbine converts the available power into useful power is 59.25%.

Maximum turbine output mechanical power available given as follow:

$$p_t = \frac{1}{2}\rho A V_w^3 C_p \tag{4.2}$$

$$C_p = \frac{P_t}{P_w} \tag{4.3}$$

Where;

P_t is the output power of wind turbine

P_w is the available or input power of wind turbine

C_p is the wind power coefficient

For a given wind turbine, if we fix the pitch angle beta at a constant value then the tip speed ratio (TSR) only determines the wind power coefficient.

The tip-speed radio (TSR) defined as:

$$\lambda = \frac{R\omega_{turb}}{V_w} \tag{4.4}$$

Where;

λ is tip speed ratio

ω_{turb} is the turbine rotational angular speed

V_w is the available wind speed

The turbine rotor torque and the power output of the wind turbine related in the equation below as:

$$T_{turb} = \frac{P_t}{\omega_{turb}} = \frac{\rho A V_w^3 C_p}{2\omega_{turb}} = \frac{\rho \pi R^3 V_w^3 C_t}{2} \tag{4.5}$$

Where;

C_t is the coefficient of torque

The coefficients of power C_p and torque C_t are related by the equation below as:

$$C_P(\lambda) = \lambda C_t(\lambda) \tag{4.6}$$

4.2.2 Mechanical Shaft and Gearbox Modeling

The DFIG based wind energy conversion system includes a gearbox, which connects the slow shaft of the turbine to the fast shaft to increase the speed of the input shaft to that required by the generator. An increase in speed is needed because wind turbine rotors, and hence main shafts, turn at a much slower speed than required by electrical generators. The gearbox model are categorized as a single mass, two mass, and three mass models based on the speed–up ratio of a gearbox and number of stages. The two mass model is developed by neglecting the moment of inertia for the shafts and the gearbox wheels because they are small compared with the moment of inertia of the wind turbine or generator. Then, the one-mass model which is obtained in this case can be described by further neglected the stiffness and the damping factor for both low speed and high-speed shafts. The equivalent physical model considered for the representation of the mechanical

transmission system dynamics shown in figure 4.1.

Then, the model of the drive system in this case is described by the following equation:

$$T_{total} = J_{toal}\frac{d\omega_m}{dt} \tag{4.7}$$

The equivalent torque, the equivalent moment of inertia and the mechanical speed given by:

$$T_{total} = T_m - T_{em} \tag{4.8}$$

$$J_{toal} = J_g + \frac{J_{turb}}{N^2} \tag{4.9}$$

$$\omega_m = N * \omega_{turb} \tag{4.10}$$

$$T_m = \frac{1}{N}T_{turb} \tag{4.11}$$

Where;

N is the gear box ratio

T_m is the torque applied to the shaft of the generator

T_{em} is the generator electromagnetic torque

T_{total} is the total torque

ω_m is the generator mechanical speed

J_{total} is the total moment of inertia

J_{turb} is wind turbine moment of inertia

J_g is the generator moment of inertia

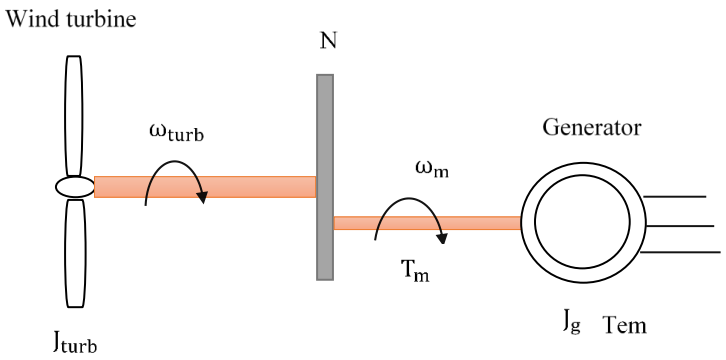

Figure 4.1: Mechanical arrangement of wind turbine drive train

4.2.3 Controller for Wind Turbine

The controller is based on the most successful control strategy named as MPPT and its objective is to rotate the turbine over a certain wind speed range in order to maintain the tip speed ratio (λ) at its optimal value λ^{opt} which makes the turbine to operate at optimum power coefficient (C_p^{opt}).

The optimum tip−speed radio (TSR) calculated as:

$$\lambda^{opt} = \frac{R\omega_{turb}^{opt}}{V_w} \tag{4.12}$$

For a wind turbine, from the mechanical modelling of the systems:

$$J_{turb}\frac{d\omega_{turb}}{dt} = T_{turb} - T_m \tag{4.13}$$

The controller of the wind turbine is achieved through controlling ω_{turb} by adjusting the electromagnetic torque of the generator (T_{em}). These is explained using maximum power point tracking controller to generate the torque reference signal T_{em}^* as bellow:

When the turbine is working on the maximum power point, the maximum turbine torque extracted by the turbine is then given by:

$$T_{turb}(\max) = \frac{\rho\pi R^3 V_w^3 C_t^{opt}}{2} = \frac{\rho\pi R^5 \omega_{turb}^2 C_p^{opt}}{2(\lambda^{opt})^3} \tag{4.14}$$

Moreover, from the mechanical modeling of the wind turbine;

$$T_m = \frac{T_{turb}}{N} \tag{4.15}$$

Substituting equation (4.14) into equation (4.15), we can get the maximum mechanical torque given by:

$$T_m(\max) = \frac{\rho\pi R^5 \omega_{turb}^2 C_p^{opt}}{2(\lambda^{opt})^3 N} = \frac{\rho\pi R^5 C_p^{opt} \omega_m^2}{2(\lambda^{opt})^3 N^3} = K_{opt}\omega_m^2 \tag{4.16}$$

Where;

$$K_{opt} = \frac{\rho \pi R^5 C_p^{opt}}{2(\lambda^{opt})^3 N^3} \tag{4.17}$$

Now set the T_{em}^* value at $T_m(max)$ such that the controller operate to extract maximum power from each variable wind speed.

4.3 Doubly-Fed Induction Generator (DFIG) Modeling

It is essential to know the DFIG dynamic modelling for the purposes of better understanding and designing control schemes for DFIG based wind turbine-generator system. The space vector model of the DFIM can be represented into both $\alpha\beta$ and dq reference frame. When the DFIG is connected to a three phase balanced supply, the relationships between voltages, currents and flux linkages of each phase of the machine on the stator and rotor side given by:

$$V_s = R_s I_s + \frac{d\Psi_s}{dt} \tag{4.18}$$

$$V_r = R_r i_r + \frac{d\Psi_r}{dt} \tag{4.19}$$

$$\psi_s = L_s i_s + L_m i_r \tag{4.20}$$

$$\psi_r = L_r i_r + L_m i_s \tag{4.21}$$

Where;

The subscript s denotes that one space vector is referred to the stator

The subscript r denotes that one space vector is reference to the stato

The symbols v,i and Ψ represent voltages, current and flux linkages respectively

R_s and R_r represent the stator and rotor winding resistances respectively

L_s represents the stator leakage inductance

L_m represents mutual leakage inductance

L_r represents the rotor leakage inductance

Modelling and analysis of voltage, current and mutual inductance in (abc) stationary

reference frame depends on time. Such system is difficult to manage and needs to convert time-variant parameters in to time-invariant by transforming them first into two-phase stationary reference frame and then transforming to an appropriate two-phase rotating reference frame.

4.3.1 Modeling in $\alpha\beta$ Stationary Reference Frame

Modeling the DFIG in $\alpha\beta$ reference frame model requires space vector theory to the basic electric equations of the machine and it resembles the dq modeling but it is stationary. Typically, three different rotating reference frames utilized to develop space vector-based models of the DFIM. The stator reference frame ($\alpha\beta$) is a stationary reference frame, the rotor reference frame (DQ) rotates at ω_m and the synchronous reference frame (dq) rotates at ω_s.

The voltage equations in equation (4.18) and (4.19) represented in to two-phase stationary reference frame ($\alpha\beta$) using the following set of equations:

$$v_{\alpha s} = R_s i_{\alpha s} + \frac{d\Psi_{\alpha s}}{dt} \tag{4.22}$$

$$v_{\beta s} = R_s i_{\alpha s} + \frac{d\Psi_{\beta s}}{dt} \tag{4.23}$$

$$v_{\alpha r} = R_r i_{\alpha r} + \omega_m \psi_{\beta r} + \frac{d\Psi_{\alpha r}}{dt} \tag{4.24}$$

$$v_{\beta r} = R_r i_{\beta r} - \omega_m \psi_{\alpha r} + \frac{d\Psi_{\beta r}}{dt} \tag{4.25}$$

Similarly, the stator and the rotor flux expressions derived in $\alpha\beta$ stationary reference frame expressed as:

$$\psi_{\alpha s} = L_s i_{\alpha s} + L_m i_{\alpha r} \tag{4.26}$$

$$\psi_{\beta s} = L_s i_{\beta s} + L_m i_{\beta s} \tag{4.27}$$

$$\psi_{\alpha r} = L_r i_{\alpha r} + L_m i_{\alpha r} \tag{4.28}$$

$$\psi_{\beta r} = L_r i_{\beta r} + L_m i_{\beta r} \tag{4.29}$$

Where;

ω_m is the rotational mechanical speed in (rad/s)

$v_{\alpha s}, v_{\beta s}, v_{\alpha r}, v_{\beta r}, i_{\alpha s}, i_{\beta s}, i_{\alpha r}, i_{\beta r}$ are voltages and currents of the stator and rotor in α and β axis

$\psi_{\alpha s}, \psi_{\beta s}, \psi_{\alpha r}, \psi_{\beta r}$ are flux linkages of the stator and rotor in α and β axis

Here we use a transformation matrix to calculate voltage and current in $\alpha\beta$ reference frame given by:

$$\begin{bmatrix} X_\alpha \\ X_\beta \end{bmatrix} = \begin{bmatrix} \cos\theta_s & \sin\theta_s \\ -\sin\theta & \cos\theta_s \end{bmatrix} \begin{bmatrix} X_a \\ X_b \\ X_c \end{bmatrix} \tag{4.30}$$

Where;

X_α and X_β represents voltage and current in $\alpha\beta$ reference frame separated by 90°

X_a , X_b and X_c represents voltage and current in abc reference frame separated by 120°

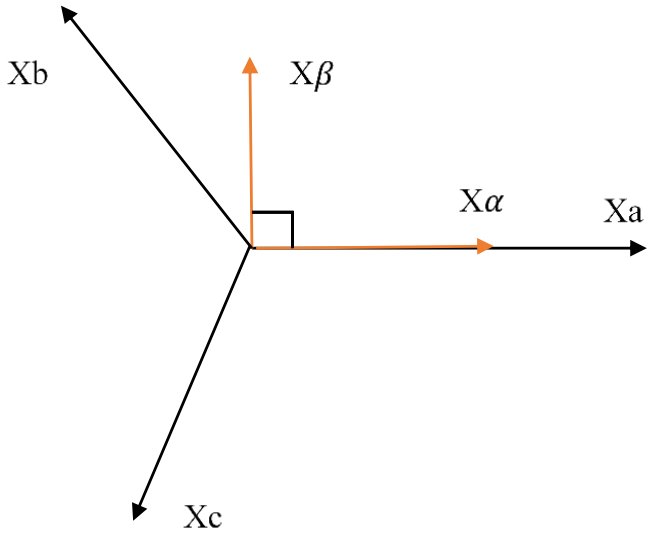

Figure 4.2: Schematic diagram of abc to $\alpha\beta$ stationary reference frame transformation

4.3.2 Modeling in dq Synchronously Rotating Reference Frame

The space vector model of the DFIM represented by defining the dq reference frame, which will be rotating at the synchronous angular speed of the system. The two-phase

synchronously rotating dq reference frame voltage equations formulated as below:

$$v_{ds} = R_s i_{ds} - \omega_s \psi_{qs} + \frac{d\Psi_{ds}}{dt} \tag{4.31}$$

$$v_{qs} = R_s i_{qs} + \omega_s \psi_{ds} + \frac{d\Psi_{qs}}{dt} \tag{4.32}$$

$$v_{dr} = R_r i_{dr} - \omega_r \psi_{qr} + \frac{d\Psi_{dr}}{dt} \tag{4.33}$$

$$v_{qr} = R_r i_{qr} + \omega_r \psi_{dr} + \frac{d\Psi_{qr}}{dt} \tag{4.34}$$

Similarly, the expression for fluxes given by:

$$\psi_{ds} = L_s i_{ds} + L_m i_{dr} \tag{4.35}$$

$$\psi_{qs} = L_s i_{qs} + L_m i_{qr} \tag{4.36}$$

$$\psi_{dr} = L_r i_{dr} + L_m i_{ds} \tag{4.37}$$

$$\psi_{qr} = L_r i_{qr} + L_m i_{qs} \tag{4.38}$$

Where;

ω_s is the angular slip frequency (rad/s)

$omega_r$ is the generator angular electrical speed in (rad/s)

$v_{ds}, v_{qs}, v_{dr}, v_{qr}, i_{ds}, i_{qs}, i_{dr}, i_{qr}$ are voltages and currents of the stator and rotor in d and q axis

$\psi_{ds}, \psi_{qs}, \psi_{dr}, \psi_{dr}$ are flux linkages of the stator and rotor in d and q axis

Here we use a transformation matrix to calculate voltage and current in d and q reference frame given by:

$$\begin{bmatrix} X_d \\ X_q \end{bmatrix} = \begin{bmatrix} \cos\theta_s & \sin\theta_s \\ -\sin\theta & \cos\theta_s \end{bmatrix} \begin{bmatrix} X_\alpha \\ X_\beta \end{bmatrix} \tag{4.39}$$

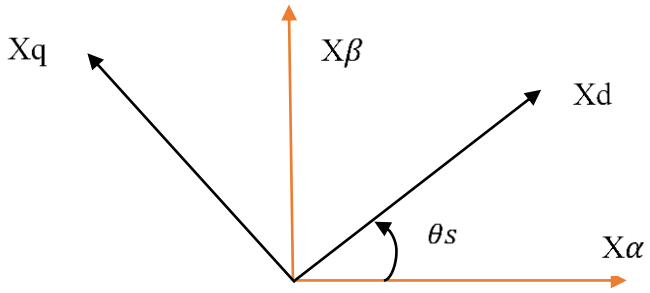

Figure 4.3: Schematic diagram of $\alpha\beta$ to dq synchronously rotating reference frame transformation

In order to align the dq reference frame with the stator flux, the angle of the stator can be calculated by representing the stator flux in the (abc) reference frame to $\alpha\beta$ stationary reference frame as:

$$\begin{aligned} \psi_s &= \psi_{\alpha s} + j\psi_{\beta s} = |\psi_s|\langle\theta_s \\ \theta_s &= \tan^{-1}\tfrac{\psi_{\beta s}}{\psi_{\alpha s}} \\ |\psi_s| &= \sqrt{{\psi_{\alpha s}}^2 + {\psi_{\beta s}}^2} \end{aligned} \tag{4.40}$$

The angle θ_s represents the location of the stator's rotating magnetic field at an instant of time.

There is a production of magnetic energy due to the mutual flux between rotor and stator, which is stored in the magnetic field. This stored energy responsible to produces an electromagnetic torque in the stator. The electromagnetic torque in the stator, the stator and rotor active and reactive powers for the DFIG represented in dq reference frame as:

$$P_s = \frac{3}{2}(v_{ds}i_{ds} + v_{qs}i_{qs}) \tag{4.41}$$

$$Q_s = \frac{3}{2}(v_{qs}i_{ds} - v_{ds}i_{qs}) \tag{4.42}$$

$$P_r = \frac{3}{2}(v_{dr}i_{dr} + v_{qr}i_{qr}) \tag{4.43}$$

$$Q_r = \frac{3}{2}(v_{qr}i_{dr} - v_{dr}i_{qr}) \tag{4.44}$$

$$T_{em} = \frac{3}{2}(i_{dr}i_{qs} - i_{qr}i_{ds}) \tag{4.45}$$

4.3.3 Control Systems for DFIG

The control of doubly fed induction generator (DFIG) completed by control of the variable frequency converter, which mainly related to the grid side and the rotor side controllers as well. Mainly the controller controls the active and reactive power in DFIG based wind energy conversion system. Among the different alternative control methods developed for the DFIG, only the vector control in synchronous reference frame strategy is chosen for implementing the control strategies for the rotor and grid side converter. The operation of vector control of the DFIG performed in a synchronously rotating dq frame, in which the d-axis is oriented with the stator flux so that the active and reactive power of the stator controlled independently by means of the quadrature and the direct current, respectively.

The control of DFIG required mainly two sub-control levels namely Rotor side converter controller and Grid side converter controller.

The objective of the RSC is to allow for decoupled controlling the active and reactive power. This facilitates high flexibility which enables the turbine to capture maximum energy from wind and to provide reactive power support to the grid. The objective of the GSC is to maintain constant voltage across the capacitor irrespective of the magnitude and direction of the rotor power.

4.3.3.1 Rotor side control

The rotor currents in abc stationary reference frame can be resolved into the quadrature (i_{dr}) and the direct current (i_{qr}) components. The direct current component produces a flux in the air gap, which is aligned with the rotating flux vector linking the stator, whereas the quadrature component produces flux at right angles to this vector. Hence $\psi_{ds} = \psi_s$ and $\psi_{qs} =$ zero.

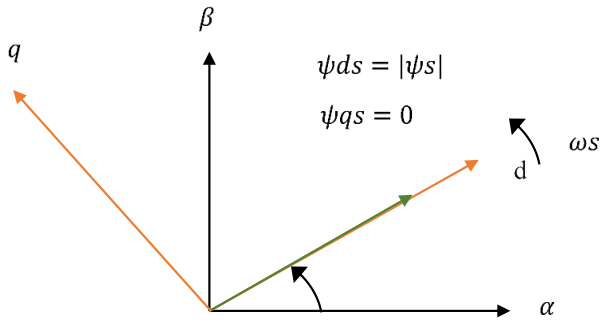

Figure 4.4: Synchronous rotating dq reference frame aligned with the stator flux space vector

Because the stator is connected directly to the grid at constant AC voltage, the stator flux is constant, and assuming that the stator resistance is small, then, the term $(\mathrm{d}\psi_{ds})/\mathrm{dt}$ and $R_s i_{ds}$ in equation (4.31) are zero. Consequently, equation (4.31) and (4.32) becomes as follows:

$$v_{ds} = R_s i_{ds} - \omega_s \psi_{qs} + \frac{d\Psi_{ds}}{dt} = 0 \tag{4.46}$$

$$v_{qs} = R_s i_{qs} + \omega_s \psi_{ds} + \frac{d\Psi_{qs}}{dt} = \omega_s \psi_s \tag{4.47}$$

Given that $\psi_{ds} = L_s i_{ds} + L_m i_{dr}$ and $\psi_{qs} = L_s i_{qs} + L_m i_{qr}$, we have:

$$i_{ds} = \frac{\psi_{ds} - L_m}{L_s} i_{dr} \tag{4.48}$$

$$i_{ds} = \frac{-L_m}{L_s} i_{qr} \tag{4.49}$$

The electromagnetic torque, active and reactive powers of the stator calculated above reduced to the equation below:

$$P_s = \frac{3}{2}\left(\frac{\psi_s \omega_{sL_m}}{L_s} i_{qr}\right) \tag{4.50}$$

$$Q_s = \frac{3}{2}\psi_s \omega_s \frac{L_m}{L_s}\left(i_{dr} - \frac{\psi_s}{L_m}\right) = K_Q\left(i_{dr} - \frac{\psi_s}{L_m}\right) \tag{4.51}$$

$$T_{em} = -\frac{3}{2} p \frac{L_m}{L_s} \psi_s i_{qr} = K_T i_{qr} \tag{4.52}$$

The above last three equations reveal that the direct rotor current is proportional to the

stator reactive power and that the quadrature rotor current is proportional to the torque and stator active power. The component i_{dr} then controls the reactive power and that of i_{qr} controls the torque or active stator power. The reference signal can be obtained from the desired electromagnetic torque (or the desired stator real power) and the desired stator reactive power, as shown below:

$$i_{qr}^{*} = \frac{2}{3}(\frac{L_s}{p\psi_s L_m})T_{em}^{*} = \frac{2}{3}\frac{L_s}{p\psi_s L_m}K_{opt}\omega_m^2 \tag{4.53}$$

$$i_{dr}^{*} = \frac{\psi_s}{L_m} + \frac{2}{3}\frac{L_s}{\psi_s \omega_s L_m}Q_s^{*} \tag{4.54}$$

The controller PI parameters are determined by comparing with the Butterworth polynomial that is described in the below section.

If we substitute equation (4.35 - 4.38) into equation (4.33) and (4.34), we have get:

$$v_{dr} = R_r i_{dr} + \sigma L_r \frac{di_{dr}}{dt} - \omega_r \sigma L_r i_{qr} + \frac{L_m}{L_s}\frac{d|\Psi_s|}{dt} \tag{4.55}$$

$$v_{qr} = R_r i_{qr} + \sigma L_r \frac{di_{qr}}{dt} + \omega_r \sigma L_r i_{dr} + \omega_r \frac{L_m}{L_s}|\Psi_s| \tag{4.56}$$

Where;

$\sigma = 1 - \frac{L_m^2}{L_s * L_r}$

The stator flux is constant and $\psi_{qs} = 0$ consequently, the term $\frac{L_m}{L_s}\frac{d|\Psi_s|}{dt}$ is zero.

If we take Laplace transform on both side of last two above equation, we can get the following equation in frequency domain as:

$$i_{dr} = \frac{v_{dr} + \omega_r \sigma L_r i_{qr}}{R_r + \sigma L_r s} \tag{4.57}$$

$$i_{qr} = \frac{v_{qr} - \sigma L_r i_{dr} \omega_r \frac{L_m}{L_s}|\psi_s|}{R_r + \sigma L_r s} \tag{4.58}$$

Let us draw the closed-loop with PI current controller of i_{dr} and i_{qr} with their respective reference value of i_{dr}^{*} and i_{qr}^{*} respectively as in the figure below:

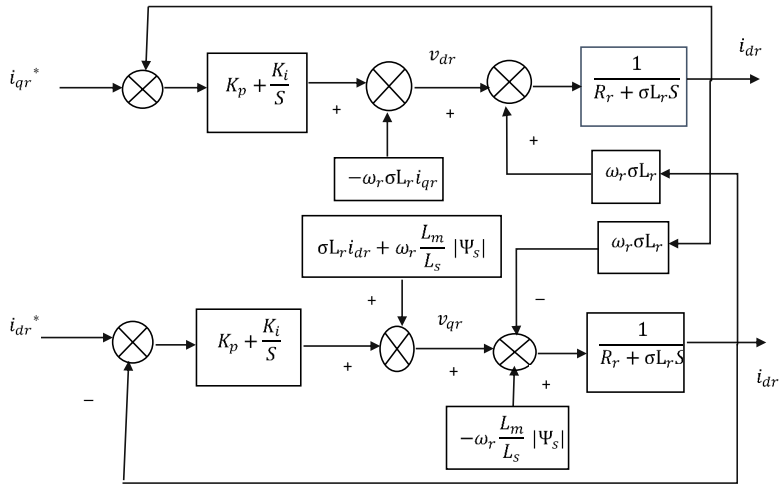

Figure 4.5: Closed loop PI current controller diagram of i_{dr} and i_{qr}

The block diagram in figure 4.5 can be reduced to a second-order closed-loop system for both currents with appropriate gain of the PI regulator as below:

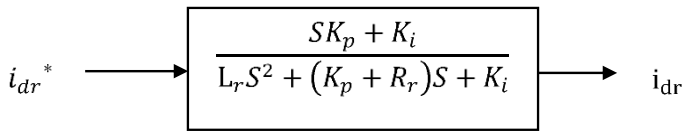

(a)

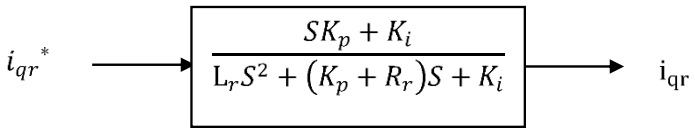

(b)

Figure 4.6: Reduced second order closed loop system (a) for i_{dr} and (b) for i_{qr}

The gain function is given by:

$$\frac{i_{dr(s)}}{i^*_{dr(s)}} = \frac{i_{qr(s)}}{i^*_{qr(s)}} = \frac{sK_p + K_i}{\sigma L_r s^2 + (K_p + R_r)s + K_i} = \frac{\frac{(sK_p + K_i)}{M}}{s^2 + \frac{(K_p + R_r)}{M} + \frac{K_i}{M}} \tag{4.59}$$

Where; $M = \sigma L_r$

The transfer function of a Butterworth polynomial of second order denominator is given

as:

$$\frac{C(s)}{R(s)} = \frac{\omega_n^2}{s^2 + 2\omega_n + \omega_n^2} \tag{4.60}$$

Where;

C(s) is out put of the transfer function

R(s) is input put of the transfer function

The controller PI parameters determined by comparing the denominators coefficient in equation (4.59) with the denominators coefficient of the Butterworth polynomial and then choosing appropriate ω_n.

Therefore;

$$2\omega_n = \frac{(K_p + R_r)}{M} \tag{4.61}$$

$$K_p = 2\omega_n M + R_r \tag{4.62}$$

$$\frac{K_i}{M} = \omega_n^2 \tag{4.63}$$

$$K_i = \omega_n^2 M \tag{4.64}$$

Where;

ω_n is the bandwidth of the current controller, which depends upon the design value

Similarly, following the procedure above, we can get a second-order closed-loop system for mechanical speed with appropriate gain of the PI regulator as below:

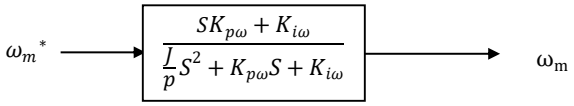

Figure 4.7: Reduced second order closed loop system for mechanical speed

Then, the PI parameters of the mechanical speed is calculated to be:

$$K_{P\omega} = \frac{J}{P} 2\omega_n \tag{4.65}$$

$$K_{i\omega} = \frac{J}{P} \omega_n \tag{4.66}$$

4.3.3.2 Grid side controller

To design the grid side controller similar to the rotor side controller the system configured by the grid side converter, filter, and grid voltage can ideally represented by the equation bellow as:

$$v_{df} = R_g i_{dg} - \omega_s L_g i_{qg} + L_g \frac{di_{dg}}{dt} + v_{dg} \tag{4.67}$$

$$v_{qf} = R_g i_{qg} + \omega_s L_g i_{dg} + L_g \frac{di_{qg}}{dt} + v_{qg} \tag{4.68}$$

Where;

V_{df} and V_{qf} are the voltage imposed by the grid side converter in α and β reference frame

V_{dg} and V_{qg} are the grid side voltage in dq reference frame

L_f is inductance of the grid side filter

R_f is resistive part of the grid side filter

In order to perform the vector control technique, the voltage along d axis of the rotating frame is aligned with the grid voltage space vector v_g as shown in Figure **??** giving the resulting dq components of the grid voltage as:

$$v_{dg} = |v_g| \tag{4.69}$$

$$v_{qg} = 0 \tag{4.70}$$

Thus, the total active and reactive powers exchanged with the grid are calculated as:

$$P_g = \frac{3}{2}(v_{dg} i_{dg} + v_{qg} i_{qg}) \tag{4.71}$$

$$Q_g = \frac{3}{2}(v_{qg} i_{dg} - v_{dg} i_{qg}) \tag{4.72}$$

Substituting the relations in equation (4.69) and (4.70) into the above last two equation; the power calculation simplified as:

$$P_g = \frac{3}{2} v_{dg} i_{dg} = \frac{3}{2} |v_g| i_{dg} \tag{4.73}$$

$$Q_g = -\frac{3}{2} v_{dg} i_{qg} = -\frac{3}{2} |v_{dg}| i_{qg} \tag{4.74}$$

The above last two equation indicate that i_{dg} control implies P_g control, while i_{qg} control implies Q_g control. The current references i^*_{dg} and i^*_{qg} are calculated from the grid side active and reactive powers as:

$$i^*_{dg} = \frac{P_g}{\frac{3}{2} v_{dg}} K_{PG} P_g \tag{4.75}$$

$$i^*_{qg} = \frac{Q_g}{-\frac{3}{2} v_{dg}} = K_{QG} Q_g \tag{4.76}$$

Where;

$K_{PG} = \frac{1}{\frac{3}{2} v_{dg}}$

$K_{QG} = \frac{1}{-\frac{3}{2} v_{dg}}$

Similar to the rotor side controller, the current i_{dg} and i_{qg} can be expressed in the frequency domain as:

$$i_{dg} = \frac{v_{df} + \omega_s L_g i_{qg}}{R_g + s L_g} \tag{4.77}$$

$$i_{qg} = \frac{v_{qf} - L_g i_{dg}}{R_g + s L_g} \tag{4.78}$$

Then parameters of the PI regulators determined by the equation below as:

$$K_{pg} = 2\omega_{ng} L_g - R_g \tag{4.79}$$

$$K_{ig} = \omega^2_{ng} R_g \tag{4.80}$$

Where;

ω_{ng} is is the bandwidth frequency of the reactive power controller

The GSC mainly controls the voltage across the capacitor and its PI parameter can be

calculated by expressing the DC voltage dynamics in DC-link as:

$$CV_{dc} = K_{vdc}(V_{dc}^{*} - V_{dc}) \tag{4.81}$$

Where;

K_{vdc} is PI controller for the DC voltage given as: $K_{vdc} = \left[K_{pv} + \frac{K_{iv}}{s}\right]$

Then, The equation (4.81) written as:

$$CV_{dc} = \left[K_{pv} + \frac{K_{iv}}{s}\right] V_{dc}^{*} - \left[K_{pv} + \frac{K_{iv}}{s}\right] V_{dc} \tag{4.82}$$

The gain function becomes:

$$\frac{V_{dc}}{V_{dc}^{*}} = \frac{\frac{1}{C}(sK_{pv} + K_{iv})}{s^2 + s\frac{K_{pv}}{C} + \frac{K_{iv}}{C}} \tag{4.83}$$

Then the PI parameter calculated to be:

$$K_{pv} = 2C\omega_{dc} \tag{4.84}$$

$$K_{iv} = C\omega_{dc}^{2} \tag{4.85}$$

Chapter 5

SIMULATION STUDIES AND RESULT ANALYSIS

5.1 System under Study

This thesis work performed on the Sheno feeder of the Debre Berhan power distribution substation and the single line schematic diagram of the substation is shown in figure 5.1 below. This chapter begins by describing the performance of the Sheno feeder without the installation of distributed generators. The total real and reactive power loading of the system is 8.0284MW and 4.7223kVAr respectively. It also presents the result obtained using HHO Simulation Algorithm. The implementation steps of the proposed algorithm is programmed using Matlab software. The obtained results subdivided into different sections depending on the number of DG being optimally placed and sized. In other words, one or more DGs have been installed in the test systems for more economic and technical benefits.

The maximum and minimum ratings of DGs are taken as 80% and 10% of total connected loads respectively [52]. All the buses are considered to be possible candidate buses for DG placement except the slack bus. The IEEE standard minimum voltage used is 0.95 and the maximum voltage is 1.05, which is ±5% compared to the rated value.. The optimum DGs power factor is determined for maximum capacity utilization and hence, optimum benefit can be extracted from DGs.

The substation supplied from 132KV grid transmission line and there is two main power transformer in the substation supplied the city with a primary voltage of 15 and

33KV. There are eight (8) radially configured feeders to distribute primary voltage level power to the distribution transformer and industrial loads. The 33KV voltage supplies four outgoing feeders, these are: Sheno2, Enwary, AliuAmba, Dashin, and 15KV side similarly have four outgoing feeders such as blanket factory, Ankober, Mendida, and Sheno.

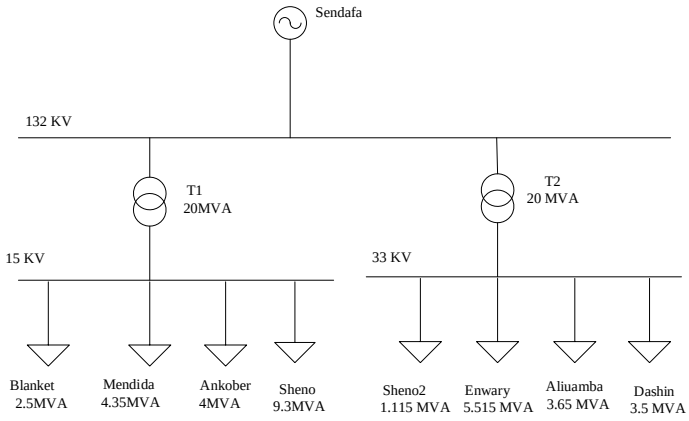

Figure 5.1: Single line diagram of Debre Berhan substation out going feeders

All required data including line resistance and load data, power interruption frequency, and duration are collected from the Debre Berhan district utility. To reduce the complexity of the analysis in the system the Sheno (15kV) feeder is selected due to:

- They fed power to all kinds of loads such as industrial, commercial, and domestic
- High numbers of customers are connected and rate of load increment is higher.
- Served more Debre Berhan town customers than the other feeders
- There is a higher imbalance between the load and supply even if the substation try to supply the load with two feeders

Table 5.1: Data for main transformer in Debre Berhan distribution substation

Transformer type	Transformer quantity	Voltage level (KV)	Transformer capacity(MVA)
Main trnasformer1	1	33	20
Main trnasformer2	1	15	20

Table 5.2: Distribution transformer and load data for Sheno feeders

Transformer KVA rating	quantity	Total number of transformer	Active power (MW)	Reactive power (MVAr)
25	4	31	8.0674	4.7223
50	2			
100	8			
200	4			
315	6			
630	1			
800	3			

5.2 Cause of Interruption in the Feeder

Among the different types of causes for power interruption, frequently occurring at Sheno feeder include component failure(CF), component maintenance(CM), line shedding, broken line, animal, wind and tree failure(W,A&T), and unkowun cause(UC) causing permanent and transient earth fault(EF), permanent and transient short circuit(SC), open circuit fault(OC) and longer interruption duration for operation and maintenance. The interruption duration is taken for one year to identify the main cause of power interruption in the feeder, the duration of the cause of faults, and the amount of energy not supplied due to interruption.

Table 5.3: Annually interruption duration and Cost of ENS for Sheno feeder

Cause of fault	Types of fault occur due to the cause								ENS (MWh)
	EF		SC		OC		OI		
	Dur (Hr.)	Freq (Int/yr.)	Dur (Hr.)	Freq (Int/yr.)	Dur (Hr.)	Freq (Int/yr.)	Dur (Hr.)	Freq (Int/yr.)	
CF	95.46	10	75.55	13	69.64	9	8.55	2	168.21
W, A & T	50.70	12	52.5	15	49.70	10	14.5	7	112.995
CM	134.87	27	115.30	11	85.80	14	20	4	355.97
UC	106.56	19	95.65	20	96.75	7	17.5	3	213.61
Total	387.6	68	339	59	301.9	40	60.5	19	850.78

The peak load of the feeder, which is 0.675 MW is used to calculate energy not supplied due to interruption in table 5.3 above.

Table 5.4: Percentage duration and frequency of each causes of fault

Cause	CF	W, A & T	CM	Unknown cause
%DR	19.77	13.28	41.84	25.11
%FR	18.78	24.31	29.83	27.07

As we observe from table 5.4, the feeder experiencing longer interruption duration and frequency of interruption due to component operation and maintenance occurred in the feeder. The total contribution of each cause for power interruption in the feeder is presented in figure 5.2 below.

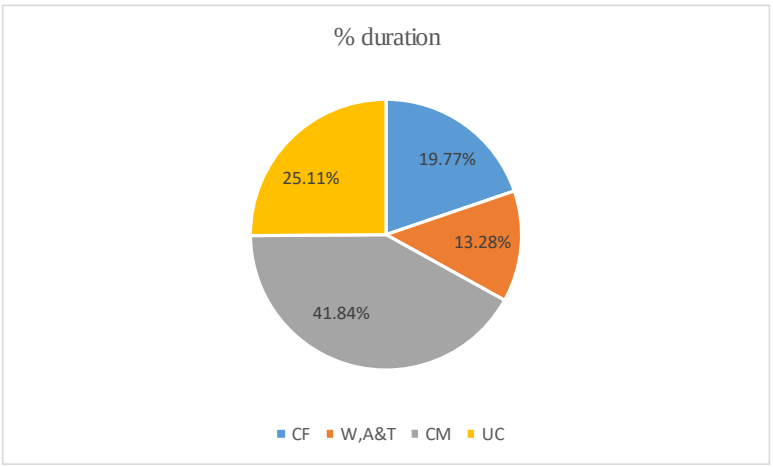

Figure 5.2: Percentage duration of each causes for power interruption

As can be seen from the chart above, 41.8 % of the interruption duration is due the component operation and maintenance, 19.77% is due to component failure, 13.28% is due to wind, animal, and tree fall. The remaining 25.11% account for unknown causes. The main cause of power interruption is component operation and maintenance. The most frequently occurred fault in the feeder is the earth fault, which accounts for 37.15% of the total interruption frequency.

Table 5.5: Percentage duration and frequency of each types of fault

Types of fault	EF	SC	OC	OI
%DR	35.6	31.13	27.72	5.6
%FR	37.15	32.24	21.8	8.7

The total percentage of frequency interruption of each fault type in the feeder is presented in figure 5.3 below.

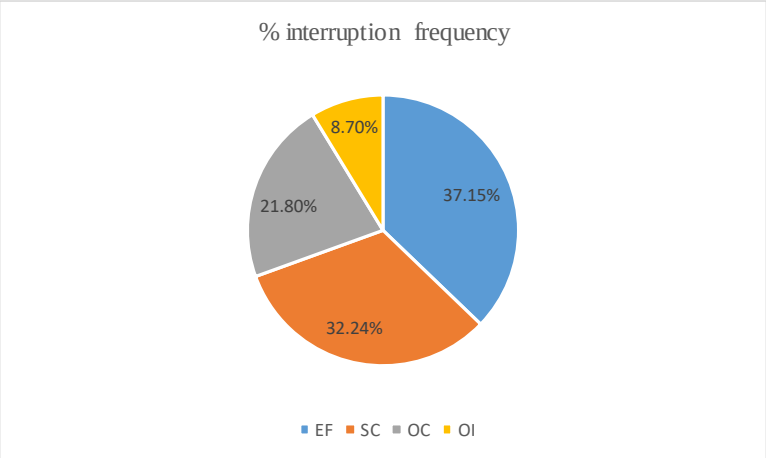

Figure 5.3: Percentage interruption frequency of each faults for power interruption

The most frequently occurred fault in the feeder is earth fault, which accounts for 37.15% of the total interruption frequency.

5.3 Simulation result for different cases

To analyze the power loss and voltage drop, the following case studies are undertaken to the Sheno feeder.

1. Base case load flow (without DG)
2. Single DG placement
3. Two DG placement

5.3.1 Results during Base case load flow (without DG)

Initially, load flow was run on the selected Sheno feeder to get the voltage at each bus, and the total power loss of the system. The system active and reactive power loss during base case load flow analysis is 1629.04KW and 609.513KVAr respectively. The total voltage drop index of the existing system is 0.4407. The bus voltage profile obtained without DG shown in table 5.6 below.

Table 5.6: Bus Voltage profile without installation of DG

Bus number	Voltage (pu)	Bus number	Voltage (pu)
1	1.0000	21	0.8581
2	0.9673	22	0.8560
3	0.9452	23	0.9295
4	0.9424	24	0.9159
5	0.9393	25	0.9068
6	0.9377	26	0.8988
7	0.9363	27	0.8907
8	0.9353	28	0.8839
9	0.9348	29	0.8781
10	0.9346	30	0.8752
11	0.9344	31	0.8738
12	0.9188	32	0.8715
13	0.9074	33	0.8708
14	0.9013	34	0.9281
15	0.8874	35	0.9270
16	0.8816	36	0.9267
17	0.8735	37	0.8529
18	0.8682	38	0.8507
19	0.8641	39	0.8500
20	0.8603	40	0.8497

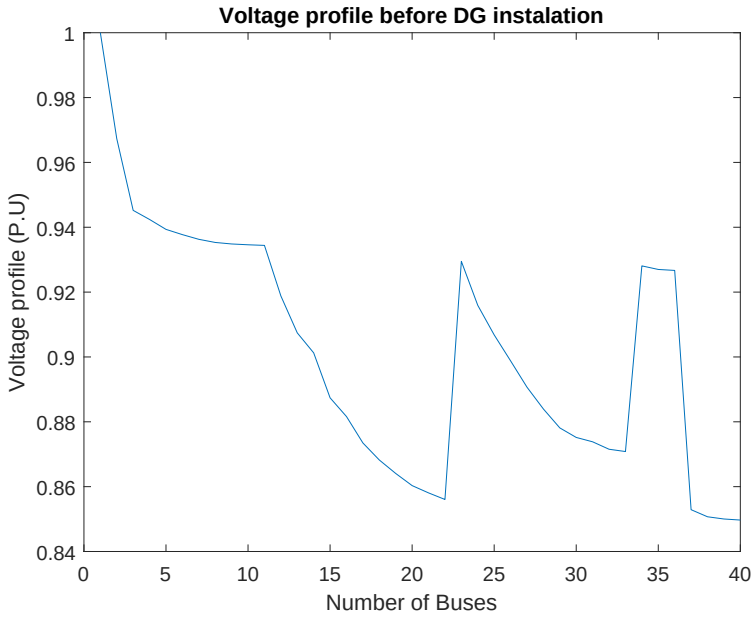

Figure 5.4: Bus voltage profile without installation of DG

Figure 5.4 shows that the voltage profile is in decreasing order starting from bus one to bus twenty-two as the resistance increases. The increasing and decreasing voltage profile at different bus shown in the figure above is due to long distribution lines, unbalance loads among the three phases, drastic increase in the load, installing a distribution transformer far from the load center.

5.3.2 Results during Single DG placement with single objective

The objective function here is only to minimize the power loss. The optimal DG size and location obtained with the proposed HHO during single DG placement with the aim of only minimizing power loss were 3.9652MW and bus 18 respectively.

The total real power loss after a single DG allocation reduced to 402.988KW. The percentage real power loss reduction is 75.26% with respect to base case loss. While that of PSO reduce the power loss to cause a 53.86%, reduction, which is an indication of HHO better performance than PSO. The base case and improved voltage magnitudes using single DG allocation with PSO and the proposed HHO were plotted against their respective bus numbers in order to see the improvement in voltage profile after single DG location and sizing.

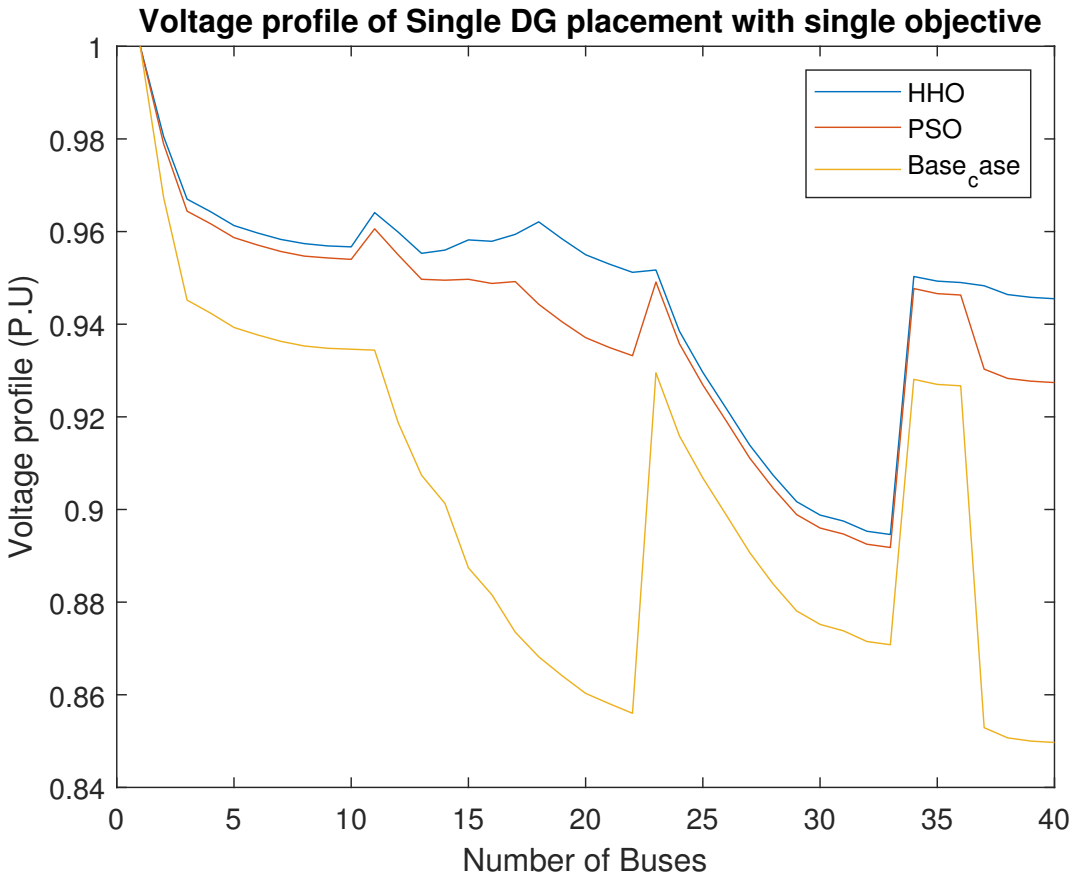

Figure 5.5: Bus voltage profile comparison with single DG installation

Figure 5.5 shows a comparison of the voltage profiles for the base case, PSO, and the proposed HHO case after a single DG allocation. The optimal allocation of single DG with HHO reduces the voltage deviation index from 0.4407 to 0.1397 causing a 68.3% improvement in the overall voltage profile of the system as compared to the base case

voltage profile. While that of PSO cause a 61.288% improvement, which is an indication of the positive effect of the DG. HHO improves the overall voltage profile of the system by 18.11% as compared to the PSO voltage profile. These all are when the single DG supplies active power only (Type one). This means the DG operated at unit power factor. When the DG supplies both active and reactive power, it operates at a power factor between zero and one. The optimal power factor is the one that gives minimum power loss at optimal DG size and location. Mostly the optimal power factor of DG lies between 0.8 and 0.9 to reduce the system loss optimally [53]. Table 5.7 shows the power loss at different power factors.

Table 5.7: Power loss at different power factor

Pf	0.8	0.81	0.82	0.83	0.84	0.85	0.86	0.87	0.88	0.89	0.9	0.91	0.92	1
loss	331	325	314	317	321.3	327	336	343.5	351	357	364	379	390	402

From table 5.7, we can determine the optimal power factor of the DG to be 0.82 as the loss start to increases below these power factor.At these power factor, the DG supplies both active and reactive power of size 3.9652MW and 2.7677KVAr respectively. In order to see the improvement in voltage profile after the optimal single DG supplies both active and reactive power (Type two DG), the bus voltage magnitudes along these two types were plotted against their respective bus numbers.

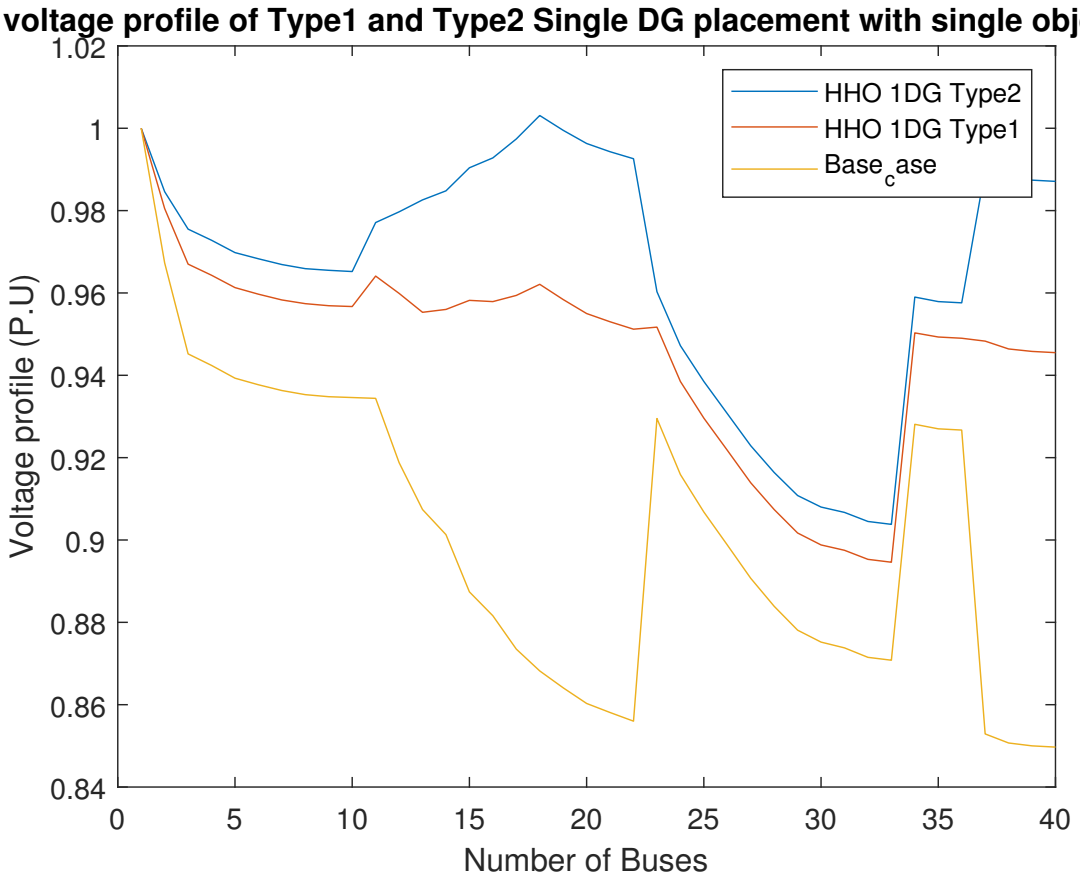

Figure 5.6: Bus voltage profile comparison between single DG of Type1 and Type2 with single objective

Figure 5.6 shows a comparison of the voltage profiles of single DG allocation for Type1, Type2, and the base case using HHO optimization. The overall voltage deviation index for the base case, Type1 and Type2 with single DG allocation using HHO is 0.4407, 0.1397, and 0.0851 respectively. These indicate single DG location of Type2 minimizes the voltage drop by 80.68% and 39.08% compared to the base case and Type1 DG respectively.

Table 5.8: Simulation results of the proposed and PSO algorithms for single DG

Methods	Type of DG	DGL	DG capacity		Power loss		%PLR	%QLR	VDI
			MW	MVAr	KW	KVAr			
	No DG	-	-	-	1629.04	609.513	-	-	0.4407
PSO	Type one	17	3.4378	-	487.00	320.449	70.11	47.43	0.1706
	Type two	17	3.4378	2.3995	381.991	218.713	76.55	64.12	0.1059
HHO	Type one	18	3.9652	-	402.988	314.098	75.26	48.47	0.1397
	Type two	18	3.9652	2.7677	314.984	213.758	80.66	64.85	0.0851

When the single DG supplies both active and reactive power, the power loss reduced by

21.83% with HHO compared to the DG supplies only active power. From the table 5.8, the percentage reduction in real power losses obtained using Type2 DG is much interest and quite important and Harris hawks optimization (HHO) shows better performance than particle swarm optimization (PSO) in reducing the total active power loss and voltage drop in the system.

5.3.3 Results during two DG placement with single objective

Results for this case are tabulated in table 5.9. For this setting, the Optimal placement and sizing of two units of DG with HHO that minimizes the power loss located at buses 17 and 25, with sizes of the DG 2.4929MW and 2.5MW respectively. Here, total real power losses reduced to 261.827KW from 1629.04KW, and consequently the reactive power reduced to 191.178KVAR from 609.513KVAr. This indicates an active power loss reduction of about 83.92% and reactive power loss reduction of 68.64 % with respect to base case loss. Similarly, PSO reduces the active and reactive power loss by 76.9% and 60.79% respectively. The bus voltage magnitude at each bus after two DG allocations with HHO, PSO, and base case system is drawn in figure 5.7 below to show the improved voltage profile compared to the base case.

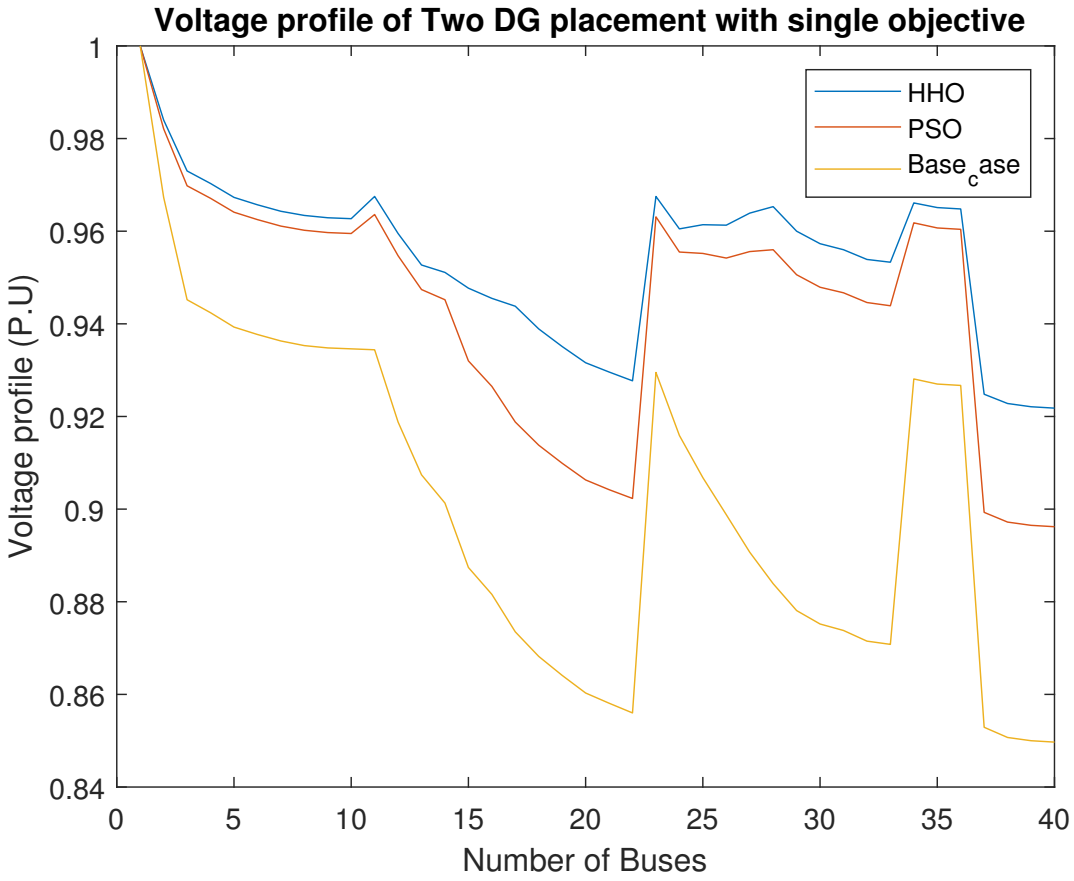

Figure 5.7: Bus voltage profile comparison of two DG single objective

Figure 5.7 above shows a comparison of the voltage profiles for the base case, PSO, and the proposed HHO case after two DG allocation considering only minimizing the power loss. Here, total VDI reduced to 0.0937 and 0.1526 with HHO and PSO respectively. These indicate that optimal allocation of two DG with PSO caused a 65.37% improvement in the overall voltage profile of the system as compared to the voltage profile of the base case while the proposed HHO cause a 78.74% and 38.59% improvement in voltage profile compared to the base case and PSO. Which is an indication of the positive effect of the DG. In order to see the improvement in voltage profile when the DG supplies both active and reactive power (Type two DG) compared to the DG supplies only active power (Type one DG) the bus voltage magnitudes along these two types were plotted against their respective bus numbers.

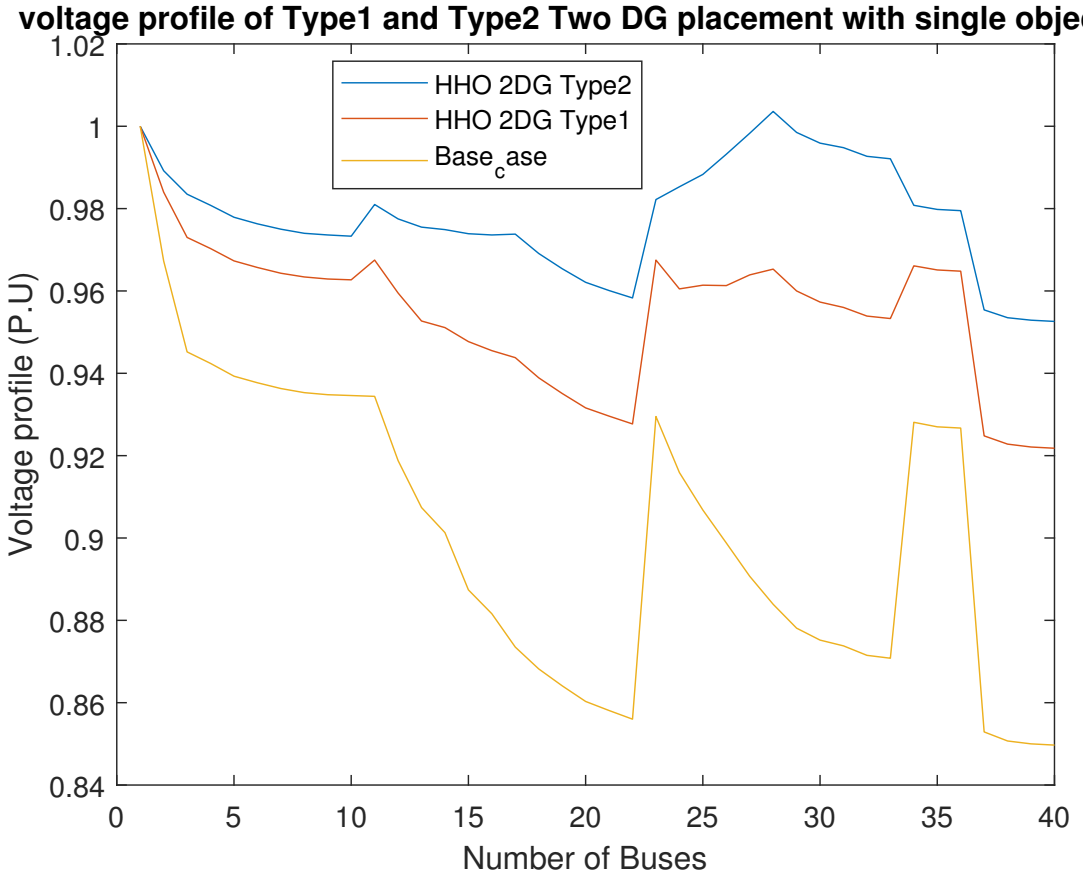

Figure 5.8: Bus voltage profile comparison between two DG of Type one and Type two with single objective

Figure 5.8 shows a comparison of the voltage profiles of two DG allocation for Type1, Type2, and the base case using HHO optimization. The overall voltage profile index for single objective two DG allocation of Type2 using HHO is 0.0263. These indicate that Type2 DG minimizes the voltage drop by 94% and 71.93% compared to the base case and Type one DG respectively.

Table 5.9: Simulation results of the proposed and PSO algorithms for Two DG Single objective

Methods	Type of DG	DGL	DG capacity		Power loss		%PLR	%QLR	VPI
			MW	MVAr	KW	KVAr			
	No DG	-	-	-	1629.04	609.513	-	-	0.4407
PSO	Type one	14 28	2.2437 2.1895	-	376.02	238.972	76.9	60.79	0.1526
	Type two	14 28	2.2437 2.1895	1.566 1.5283	98.2359	44.833	83.96	86.93	0.0189
HHO	Type one	17 28	2.4927 2.500	-	261.827	191.178	83.92	68.64	0.0937
	Type two	17 28	2.4927 2.500	1.7398 1.7450	113.406	76.8894	93.04	89.92	0.0263

When the optimal two DG supplies both active and reactive power, the power loss reduced by 93.04% and 56.68% with HHO compared to the system without DG, and the DG supplies only active power respectively. The proposed HHO reduced the power loss by 30.37% compared to PSO during two DG locations in the system. This indicates that Harris hawks optimization (HHO) shows better performance than particle swarm optimization (PSO) in reducing the total active power loss and voltage drop in the system with two DG system similar to a single DG location.

5.3.4 Results during Two DG placement with multi objective

For this scenario, objectives P_L,Q_L,C_{DG}, and VDI are considered for minimization by optimal placement of two DGs. Therefore, the system will have minimum active and reactive power loss with lesser DG cost and voltage drop simultaneously after penetrations. The optimum result in these case is tabulated in table 5.10. As mentioned in chapter three, the allocation of the various weights in a given multi-objective function varies according to the engineer's concern. In this thesis work, more emphasis is given to real power loss reduction since this results in a considerable decrease in total cost of operation and this is not to mean that the other three factors are not important. Thus taking this into consideration a study of the effect of the weights on the fitness was done so as to determine the best weights combination to adopt in coming up with the multi-objective function. During this study, the values of the weights were assumed positive and restricted

as follows:

Table 5.10: Multi objective Weight factors

K1	K2	K3	K4	Fitness
0.6	0.2	0.1	0.1	0.1443
0.6	0.1	0.2	0.1	0.1371
0.6	0.1	0.1	0.2	0.1515
0.7	0.1	0.1	0.1	0.1521

From the table 5.10 above, the combination of weights chosen is the one that gave the minimum best fitness. Thus, the weights chosen were; K1=0.6, K2=0.1, K3=0.2, K4=0.1 and the multi-objective function given by equation becomes:

$$MOF = 0.6 * PLRI + 0.1 * QLRI + 0.2 * VPII + 0.1 * ACRI \tag{5.1}$$

During the MOF case, the minimum power loss obtained is 290.097 KW that is slightly greater than the single-objective case. This is due to the way of searching the optimal location and size not only to minimize the active power loss but also reactive power loss, voltage drop, and annual cost of operation. In order to see the performance of HHO compared to PSO and the improvement in voltage profile after two DG locations and sizing the base case and bus voltage magnitudes with two DG in multi-objective were plotted against their respective bus numbers.

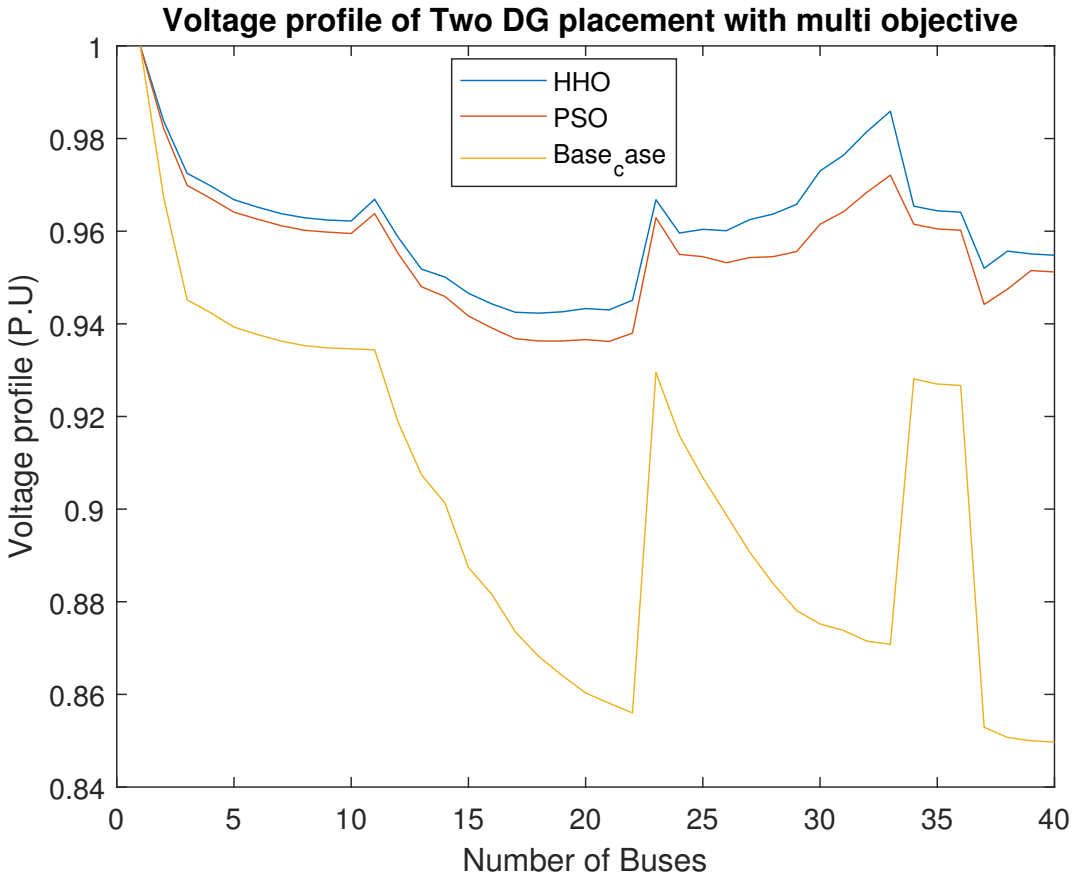

Figure 5.9: Bus voltage profile comparison with Two DG multi objective

Figure 5.9 shows the voltage profiles with the proposed HHO and PSO after two DG allocation with multi-objective compared to the base case. The optimal allocation of two DG with HHO reduce the voltage drop index to 0.0664 from 0.4407 causing an 84.93% improvement in the overall voltage profile of the system as compared to the voltage profile of the base case and 29.13%, improvement compare to the optimal allocation of trwo DG with HHO with single objective. This is an indication of the positive effect of considering voltage profile improvement in the objective function.

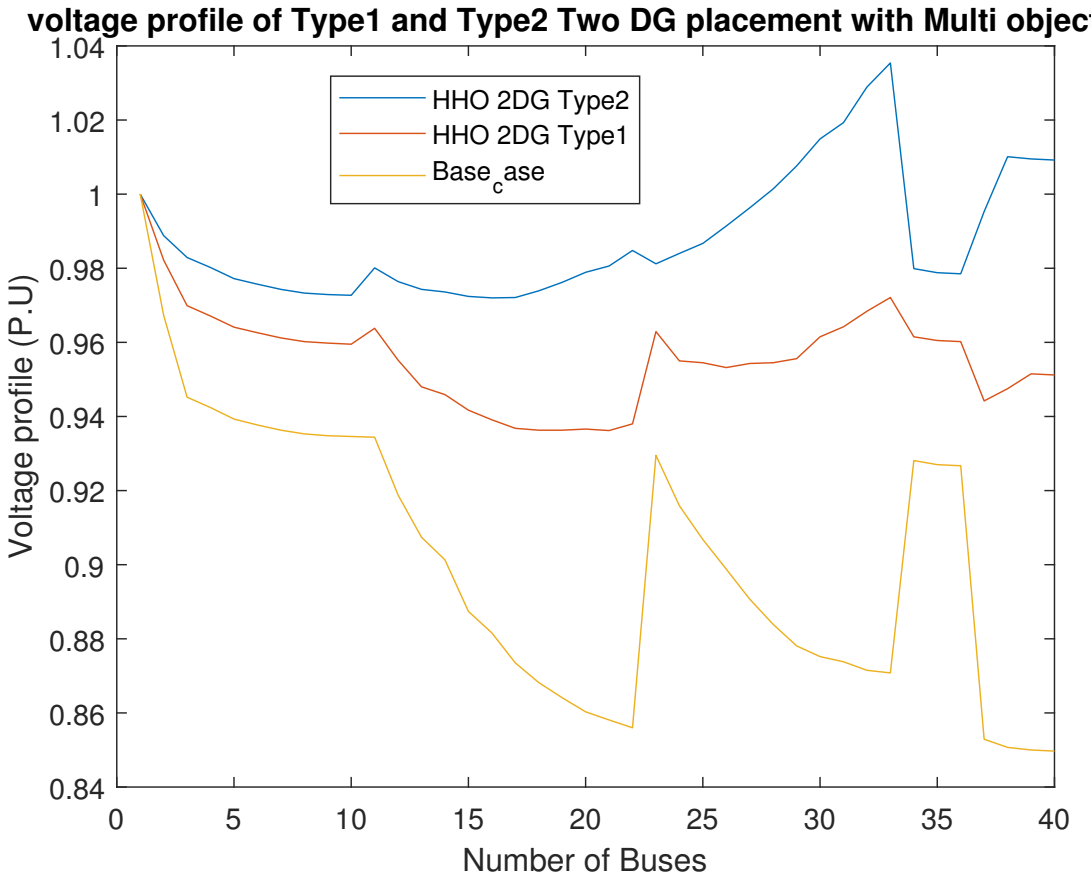

Figure 5.10: Bus voltage profile comparison between Two DG of Type one and Type two with Multi objective

The overall voltage profile with HHO during two DG Type one multi-objective is 0.0664 while during two DG Type two multi-objective case the overall voltage profile is 0.0169, which indicates an improvement of 74.54 %. Two DG multi-objective of Type two also reduce the power loss to 106.39 KW which is 63.3% reduction compared to two DG Type one multi objective.

Table 5.11: Simulation results of the proposed and PSO algorithms for Two DG multi objective

Methods	Type of DG	DGL	DG capacity		Power loss		%PLR	%QLR	VDI
			MW	MVAr	KW	KVAr			
	No DG	-	-	-	1629.04	609.513	-	-	0.4407
PSO	Type one	33 39	2.1416 2.2960	-	385.143	251.899	76.35	58.67	0.085
	Type two	33 39	2.1416 2.2960	1.6008 1.6665	188.147	152.802	88.45	74.91	0.0233
HHO	Type one	33 38	2.4997 2.4896	-	290.097	254.925	82.19	58.18	0.0664
	Type two	33 38	2.4997 2.4896	1.7447 1.7377	106.39	161.97	93.46	73.56	0.0169

5.3.5 Results during ten years forecasted load

All the above analysis is considering the existing system of Sheno feeder. The load demand in our country increases day to day. To satisfy the future demand and to make important decision on generating electric power, load switching, and infrastructure development, load forecasting is required. This paper considers Weighted Moving Average (WMA) model for solving the long-term electricity-forecasting problem as it is effective and simple to implement. This average is calculated by multiplying each of the previous yearly data by weight. The more recent values are more heavily weighted than values further in the past. The working principle of the WMA is codede in matlab to analysis the result.

Table 5.12: Simulation results for the ten years forecasted load with the proposed HHO

Years	FL (MW)	DG Location	DG Size	PLWODG (KW)	PLWDG (KW)	%PLR	VDI
2014	8.832	17	2.54	1765.57	450.52	74.51	0.114
		18	2.68				
2015	9.412	14	2.67	1894.82	315.72	83.34	0.093
		19	2.84				
2016	9.835	18	2.91	2154.53	524.12	75.67	0.0831
		27	2.85				
2017	10.874	17	3.21	2361.82	351.73	85.11	0.073
		28	2.95				
2018	11.204	19	3.46	2421.42	233.86	90.37	0.058
		33	2.87				
2019	11.473	18	3.51	2732.04	288.25	89.45	0.055
		31	3.10				
2020	11.753	14	3.25	2854.31	380.31	86.68	0.063
		23	3.63				
2021	12.681	33	3.55	3041.73	635.17	79.12	0.101
		38	3.76				
2022	13.418	28	3.71	3256.37	287.64	92.01	0.037
		35	3.82				
2023	13.75	19	4.25	3673.74	250.15	93.20	0.017
		33	3.69				

From the table we can see that the load is in increasing order and proportionally the amount of DG capacity required increases to make optimal operation in the feeder.
The voltage profile of the existing system is compared with the load profile of the feeder after ten years. The voltage profile of the feeder after ten year is more distorted compared to the existing system. After integrating DG to the system, it becomes nearly optimal.

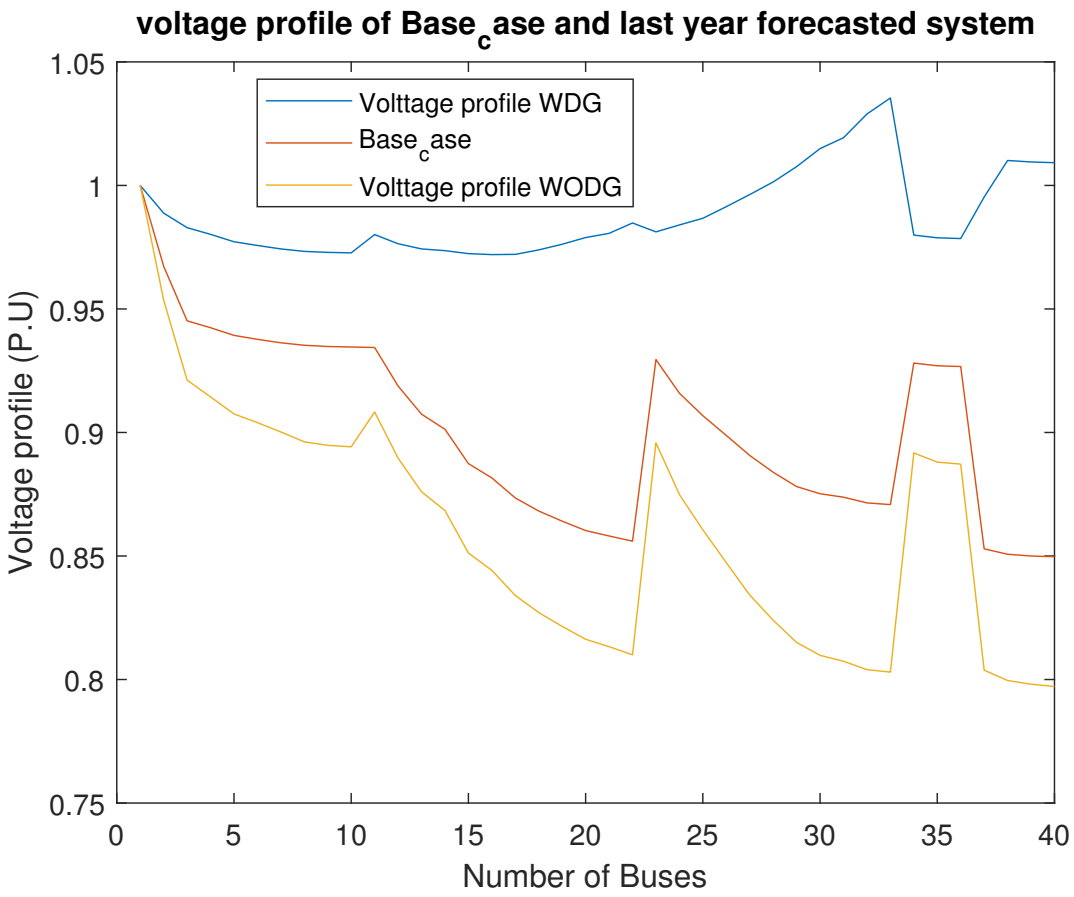

Figure 5.11: Bus voltage profile comparison between Basecase and ten years forecasted load

5.4 Cost analysis

This paper focuses on minimizing the economic operation of the distribution network due to distributed generation. Network simulation studies have been carried out on distribution systems to which single and two DGs have been connected. It is true that transmission network losses, maintenance, and operational cost have reduced with increased penetration of DGs to the system while distribution network losses are dependent on the amount of DG capacities connected to the distribution network. In general, there is a reduction of network losses, power outage duration, maintenance and operational costs when the overall network is considered thereby giving financial benefit from DGs added to the system. However, in this cost analysis, the economic loss due to transmission power loss, transmission and distribution maintenance, and operational cost are not considered due to there is no relevant data. Considering these the cost saved due to minimizing the loss for the whole case above is described in table 5.13 bellow. The revised current tariff of Ethiopian Electric Utility is used to calculate the power loss cost of the system [54].

The average of the general tariff is calculated from the revised tariff to be 1.75 Birr/kwh. The American Wind Energy Association (AWEA) explained the cost of power injected by DGs is taken as $ 1200 per KW (42000 Birr per KW) that includes capital investment for DG units with installation, operation, and maintenance cost and the average wind DG life is taken as 25 years.

Table 5.13: The economic evaluation of the optimal distributed generation

Case	Methods	PL (KW)	DG Size (KW)	DG annual Investment cost	Total annual economic loss (Birr)	Total annual economic saving (Birr)
Base case		1629.04	-	-	24,973,183	-
Single DG	PSO	381.991	3437.8	5,775,504	11,630,031	13,343,152
	HHO	314.981	3965.2	6,661,536	11,475,156	13,498,027
Two DG	PSO	188.14	2141.6 2296.0	7,455,168	10,339,354	14,633,829
	HHO	106.39	2465.8 2489.0	8,322,720	9,953,678	15,019,504

From table 5.13 the annual cost saving using integration of two DG is better than integrating a single DG in the feeder. The average annual energy not supplied due to outage and interruption of the line is 850.8MWh, which corresponds to an annual economic loss of 1,488,900 Birr. The DG supply the feeder during power outage and minimize such economic loss due to power interruption.

5.5 Simulation results of Generating optimal DG size from DFIG based Wind Energy System

The simulation is conducted based on a doubly fed induction generator based wind energy system in MATLAB/SIMULINK to generate the optimal DG size and to evaluate the performance of the vector-controlled system. The simulation does not consider the start-up of the DFIG system.

The DFIG required to generate generate nearly 2.5MW that is the optimal size of DG

determined using the proposed optimization techniques. The synchronous speed of the DFIG is 1500rpm. The generator rotates nearly at 900rpm when the available wind speed is between 5m/s and 7m/s and it operates beyond the synchronous speed when the available wind speed is between 12m/s and 15m/s.

All the results figure out here are after the system reaches a steady-state in super-synchronous modes of operation. We know that DFIG supplies the grid through both the stator and rotor. Therefore, 2MW DFIG means it deliver this power to the grid through the stator only. The total rated power (p_{mec}) generated by the wind turbine is the sum of the power through the stator and rotor.

The optimal DG size determined is nearly 2.5MW; therefore, the rating of the wind turbine selected is 2.5MW. Then the power delivered through the rotor (p_r) is 0.5MW assuming loss in the system zero.The simulation is performed at a unit power factor supplying zero reactive power ($Q = 0$) to the grid. The simulation results in the super-synchronous mode obtained by applying a wind speed of 12.5m/s which fed a speed of 1800rpm into the speed control loop of the rotor doubly fed induction generator is presented in the figure below:.

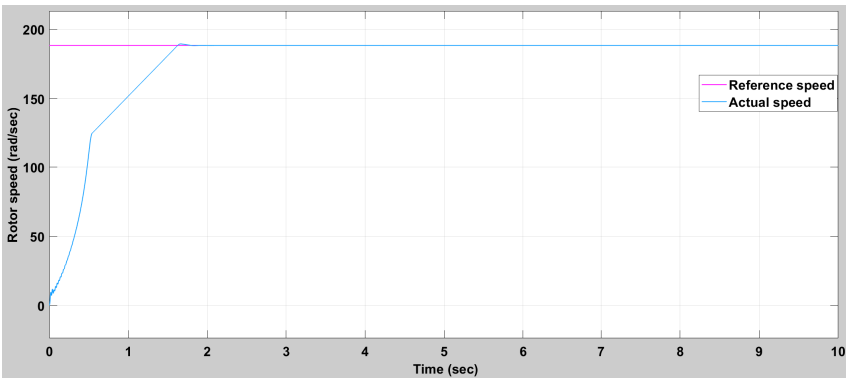

Figure 5.12: Simulated rotor speed

Figure 5.12 above demonstrates the ability of the speed control of the DFIG to maintain the specified speed at the reference signal

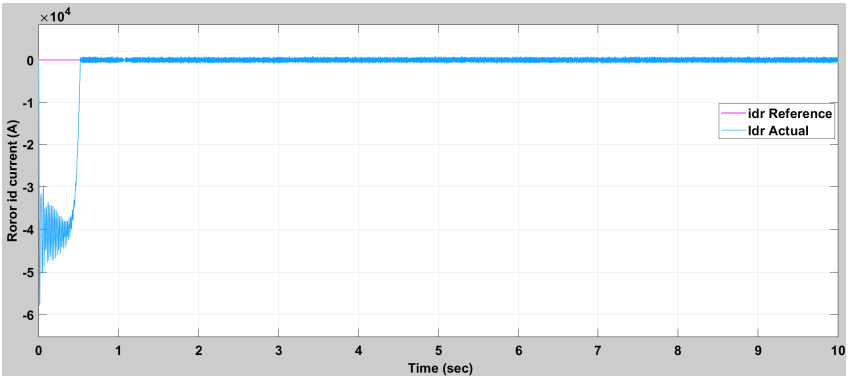

Figure 5.13: Simulated rotor id currents

The rotor id current in figure (5.13) maintained at zero value all the time since the simulation is performed at unit power factor and the corrosponding rotor vd voltage will be zero.

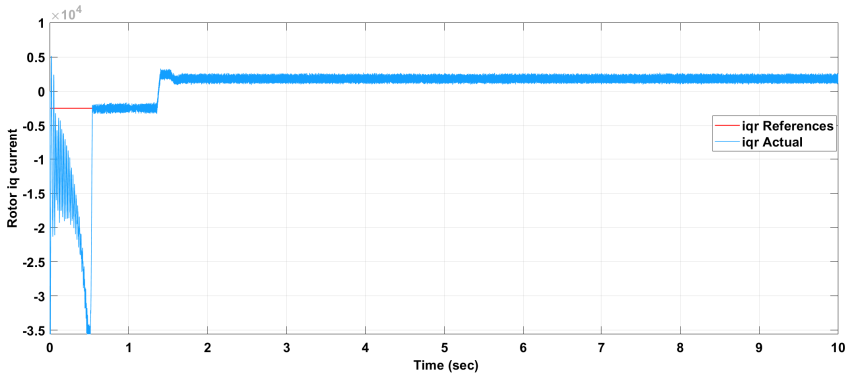

Figure 5.14: Simulated rotor iq currents

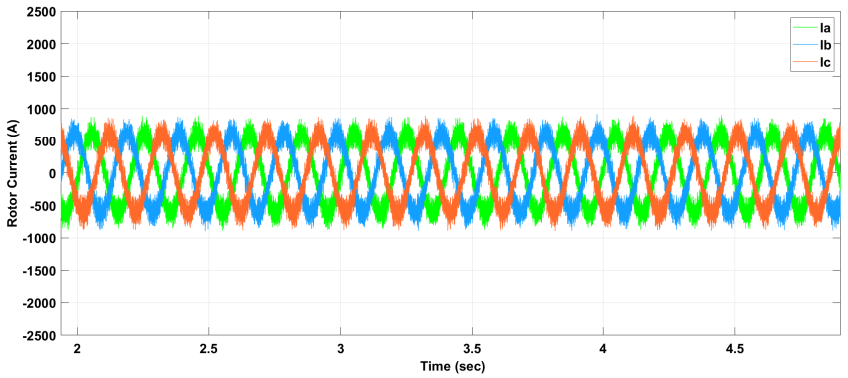

Figure 5.15: Simulated rotor three phase currents

Figure 5.14 above is the three phase current of the rotor and its frequecy is the slip time the frequency of the stator current that is 50 Hertz in this analysis. Its magnitude is nearly equal to the rotor iq current as the rotor id current is zero.

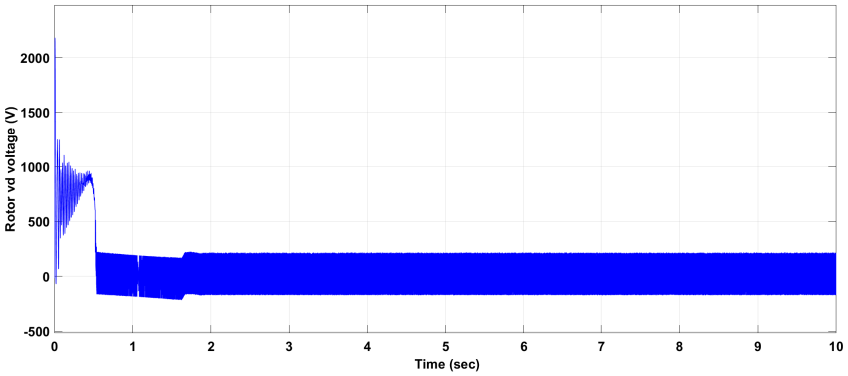

Figure 5.16: Simulated rotor vd voltage

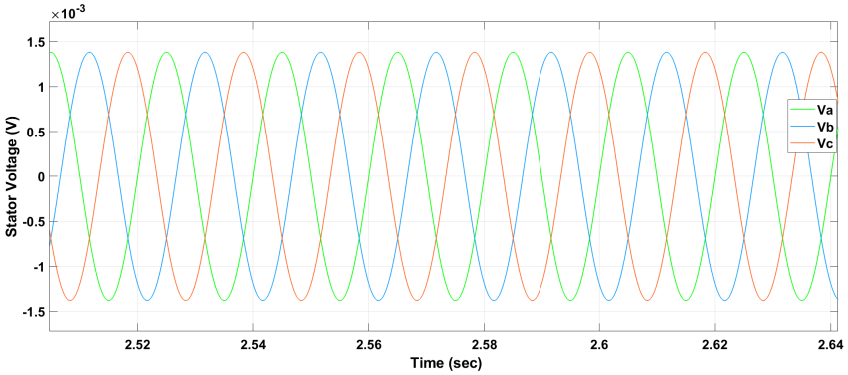

Figure 5.17: Simulated stator three phase voltage

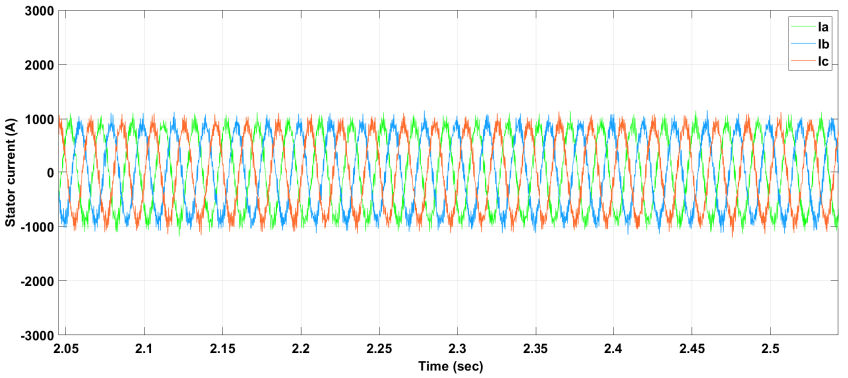

Figure 5.18: Simulated stator three phase current

Figure 5.17 and 5.16 are the three phase current and voltage respectively supplied to the stator of the DFIG from the grid.

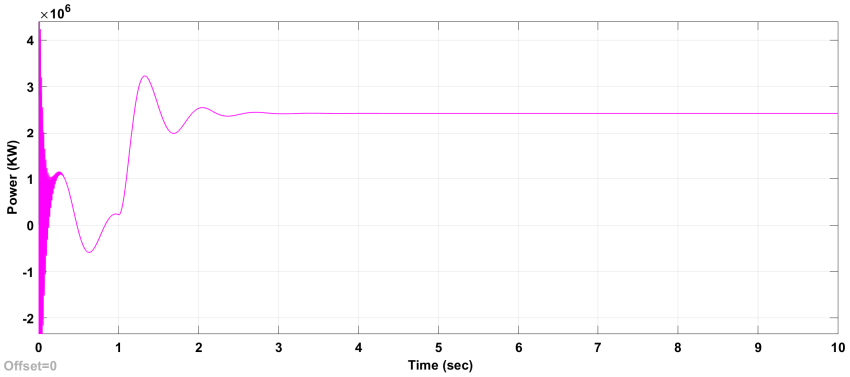

Figure 5.19: Simulated power delivered to the grid

figure 5.18 shows the total power which is nearly the optimal size of DG deliverd to the grid through the doubly fed induction generator.

Chapter 6

Conclusion and Future Work

6.1 Introduction

This chapter presents a summary of this thesis work. Mainly the chapter highlighted the general conclusion, recommendation, and suggestions for further works.

6.2 Conclusion

This research work showed the formulation of main equations of electrical power systems for power flow analysis and the formulation and implementation of the Harris hawks optimization algorithm. The algorithm helps in reducing system power losses and improving the voltage profile by optimizing the location and size of multi-type DGs. The power loss, voltage deviation, and economic cost reduction index used effectively in reducing the search space for the algorithm.

The results obtained were compared with those obtained using the particle swarm optimization algorithm. For the selected feeder, the particle swarm optimization found the optimal DG location to be bus 33 and 39 with a size of 2.1416 MW and 2.296 MW respectively. The power loss reduced to 188.147 KW considerind the DG supplies both active and reactive power to the grid. This is 88.45% total loss reduction in the feeder. The proposed HHO found the optimal DG location to be 33 and 39 with a size of 2.4997 MW and 2.4896 MW respectively.The power loss reduced to 106.39 KW which is a 93.46% total loss reduction in the feeder. Similarly, the voltage profile improved as well. Furthermore, the proposed HHO had a higher performance than the PSO method in order to calculate the optimal size and location of DG.

This thesis also studied firstly energy sources in the area and deals with modeling a generation system based on wind renewable energy. Finally, the paper explained the generation of the determined DG size from wind distributed generation.

6.3 Beneficiaries of this work

Different parties benefit from this research work both directly and indirectly. Distribution utility and customers are the direct beneficiaries of this research work. Some of the direct benefits from this work includes:

- This thesis paper will help the distribution companies in reducing both real and reactive power losses in their networks that enable them to avoid some of the penalties and compensations they incur and hence result in an improvement in annual profit.
- This paper guide the distribution company to incorporate renewable distributed generation into the distrbution network.
- Both the utility and the customer save theire materials from damege caused by voltage deviation.
- The electric tarif will be reduced due to the reduction of much investment cost in long transmission and distribution sytem.

6.4 Recommendations

Considering the cause that makes difficulties in the analysis and the result of the studies carried out in this thesis, the following points are recommended:

- We strongly recommend that EEP must consider the option of using distributed generation such that the utility company can save cost, increase transmission efficiency and reduce socio-economic problem.
- It was difficult to identify each load point and the corresponding data of that load point. This made the analysis in this thesis to be difficult. So, we recommend to EEU and power distribution substation to distinguish each load point and their corresponding failure data.

6.5 Future Works

The following items provide a shortlist of potential for future work:

- The hypred optimization with the proposed HHO algorithm can be developed for optimal DG allocation using other optimization methods such as Particle Swarm Optimization technique, Greedy Search Algorithm, and Genetic algorithm.
- Further analysis can also be done by using the developed model to simultaneously allocate more than two DG in radial distribution networks with minimum economic cost.

References

[1] Thomas Ackermann, Goran Andersson, Lennart Soder "Distributed Generation: a definition," Electric Power Systems Research, Vol.57, pp.195-204, 2001.

[2] O. A. Zongo and A. Oonsivilai, "Optimal placement of distributed generator for power loss minimization and voltage stability improvement", Energy Procedia, Vol.138, pp.134-139, 2017.

[3] U. Sultana, A. B. Khairuddin, M. M. Aman, A. S. Mokhtar, and N. Zareen, "A review of optimum DG placement based on minimization of power losses and voltage stability enhancement of distribution system," Renewable and Sustainable Energy Reviews, Vol. 63, pp. 363-378, 2016.

[4] K. Balamurugana , Dipti Srinivasana, Thomas Reindlb, "Impact of Distributed Generation on Power Distribution Systems," Energy Procedia, Vol. 25, pp. 93 – 100, 2012.

[5] H. Doagou-Mojarrad, G. B. Gharehpetian, H. Rastegar, and J. Olamaei, "Optimal placement and sizing of DG (distributed generation) units in distribution networks by novel hybrid evolutionary algorithm," Energy, Vol.54, pp. 129-138, 2013.

[6] Sarfaraz Nawaz, Sonali Singh, Supriya Awasthi, " Power Loss Minimization in Radial Distribution System using Multiple DG Units and Network Reconfiguration," European Journal of Scientific Research, Vol. 148, no 4, pp. 474-483, March, 2018.

[7] Krischonme Bhumkittipich and Weerachai Phuangpornpitak," Optimal Placement and Sizing of Distributed Generation for Power Loss Reduction using Particle Swarm Optimization," Energy Procedia, Vol. 34, pp. 307 – 317, 2013.

[8] Binayak Bhandar et al, "Optimization of Hybrid Renewable Energy Power Systems" International Journal of Precision Engineering and Manufacturing-Green Technology Vol. 2, no. 1, pp. 99-112, Jan 2015.

[9] Ruhaizad Ishak et al, "Optimal DG Placement and Sizing for Voltage Stability Improvement Using Backtracking Search Algorithm," Conference on Artificial Intelligence,

Energy and Manufacturing Engineering, June 9-10, 2014.

[10] Zhang Xiaozhao, Duan Jiandong, Han Yuhui, "Locating and Sizing of Dispersed Wind Generation in Active Distributed System," IEEE PES Asia-Pacific Power and Energy Conference, pp. 1872 –76, 2016.

[11] Atthapol Ngaopitakkul et al, "A Reliability Impact and Assessment of Distributed Generation Integration to Distribution System ," Energy and Power Engineering, Vol. 5, pp. 1043-1047, 2013.

[12] M. Esmaeilzadeh, I. Ahmadi and N. Ramezani, " Optimal Distributed Generation Planning in Radial Distribution Networks Considering Protection Coordination Limits," Iranian Journal of Electrical & Electronic Engineering, Vol. 14, no. 2, Jun 2018.

[13] Nafar M, "Optimal placement of DGs in distribution systems considering voltage stability and short circuit level improvement using GA," J Basic Appl Sci Res, Vol. 2, no. 1, pp. 368–75, 2012.

[14] Nafar M, "PSO-based optimal placement of DGs in distribution systems considering voltage stability and short circuit level improvement" J Basic Applied Science Res, Vol. 2, no. 1, pp. 703–9, 2012.

[15] Moradi MH, Abedini M, "A combination of genetic algorithm and particle swarm optimization for optimal DG location and sizing in distribution systems," Electric Power Energy System, Vol. 34, pp. 66–74, 2012.

[16] A. F. A. Kadir et al, "An improved gravitational search algorithm for optimal placement and sizing of renewable distributed generation units in a distribution system for power quality enhancement," Journal of Renewable and Sustainable Energy, Vol. 6, no. 3, 2014.

[17] Biswas S, Goswami SK, Chatterjee A. Optimum distributed generation placement with voltage sag effect minimization. Energy Convers Manage, Vol.53, no.1, pp.163–74, 2012.

[18] A. M, Abdrabou Ahmed "Voltage sag Mitigation by Optimizing the location of Distributed Generation using Genetic Algorithm for three distributed generation types," Master of Engineering (Electrical), May 2014.

[19] G. Pepermans et ai, "Distributed generation: definition, benefits and issues," Energy Policy, Vol. 33, pp.787–798, 2005.

[20] Ali M. ELTAMALY et al, " Impact of Distributed Generation (DG) on the Distribu-

tion System Network," International Journal of Engineering Science, April 2019.

[21] Dr. Mounir Bouzguenda, Abdullah Samadi, S. RajaMohamed, "Optimal Placement of Distributed Generation in Electric Distribution Networks," Ieee International Conference on Intelligent Techniques in Control, Optimization and Signal Processing, 2017.

[22] Onwunta Emea Kalu Onwunta, "Modelling and Simulation of the Impacts of Distributed Generation Integration into the Smart Grid", Ph.D Dessertation, Cape Peninsula University of Technology, Nov 2014.

[23] Diagram of geothermal power plant, MULTIMEDIA, Retrieved from http://www.eniscuola.net/en/r of-a-geothermal-power-plant.

[24] Fuel cell, WIKIPEDIA, Retrieved from, https://en.wikipedia.org/wiki/Fuel cell, Nov 2020.

[25] Biomass For Electricity Generation, WBDG, Retrieved from, https://www.wbdg.org/resources/bion electricity-generation, 09-15-2016. [26] L. Priyadarshanee, "modeling and control of hybrid ac/dc micro grid," Rourkela, 2012.

[27] Solar (PV) cell module, Samlex solar, retrieved from, https://www.samlexsolar.com/learning-center/solar-cell-module-array.aspx.

[28] Flow-Diagram-of-a-Wind-Turbine-System, retrieved from, https://www.researchgate.net/figure/Flo Diagram-of-a-Wind-Turbine-System.

[29] A. M. Eltamaly, Y. S Mohamed, A. H. M. el-sayed, and A. N. A. elghaffar, "impact of distributed generation (dg) on the distribution system network," International Journal of Engineering, April, 2019.

[30] Jhansi S, "Effects of Distributed Generation on Electrical Power Network and Protection," Journal of Electrical & Electronic Systems, Vol. 8, no 1, pp.1-3, 2019.

[31] A Hasibuan, et al, "Effect of distributed generation installation on power loss using genetic algorithm method," IOP Conf. Series: Materials Science and Engineering, Vol.308, pp.1-11, 2018.

[32] Angel Fernández Sarabia, "Impact of distributed generation on distribution system," MSC dissertation, Faculty of Engineering Science and Medicine, Aalborg University, June 2011.

[33] P. P. Barker and R. W. de Mello,, "Determining the impact of distributed generation on power systems. Part l radial distribution systems," Power Engineering Society Summer Meeting, 2000.

[34] Kumaraswamy, B. Venkataprasanth and S.Tarakalyan, "Role of Distributed Generation in Voltage Stability Enhancement," International Journal of Current Engineering and Technology, Vol.4, No.1, Feb 2014.

[35] Jinsong Liu , Junyang Zhang , Da Zhang, "Effect of Distributed Generation on Power Supply Reliability of Distribution Network," International Conference on Grid and Distributed Computing, pp. 32-35, 2015.

[36] Sanaullah Ahmad, Sana Sardar," Impact of Distributed Generation on the Reliability of Local Distribution System", (IJACSA) International Journal of Advanced Computer Science and Applications, Vol. 8, no. 6, July 2017.

[37] A.F. Abdul Kadir, A. Mohamed , H.Shareef,"Harmonic Impact of Different Distributed Generation Units on Low Voltage Distribution System," IEEE International Electric Machines & Drives Conference (IEMDC), pp.1201-1206, 2011.

[38] N. Rugthaicharoencheep, S. Auchariyamet , "Technical and Economic Impacts of Distributed Generation on Distribution System," International Journal of Electrical, Computer, Energetic, Electronic and Communication Engineering, Vol.6, no.4, 2012.

[39] M. Al-Muhaini and G. T. Heydt, "Evaluating future power distribution system reliability including distributed generation," IEEE Transactions on Power Delivery, vol. 28, no. 4, pp. 2264–2272, 2013.

[40] Pathomthat Chiradeja, "An Approach to Quantify the Technical Benefits of Distributed Generation," IEEE TRANSACTIONS ON ENERGY CONVERSION, Vol. 19, no. 4, Dec 2004.

[41] G. Pepermans, J. Driesen, D. Haeseldonckx, W. D'haeseleer and R. Belmans, "DISTRIBUTED GENERATION: DEFINITION, BENEFITS AND ISSUES," Article in Energy Policy, April 2005.

[42] Ozge Akkus and Emre Demis, "Comparison of some classical and meta–heuristic optimization techniques in the estimation of the logit model parameters," International Journal of Advanced Research, Vol.4, No.1, Oct 2016.

[43] John McCall, "Genetic algorithms for modelling and optimisation," Journal of Computational and Applied Mathematics, Vol.184, pp.205-222 2005.

[44] T. Monish kumar1, Dr V. Ganesh," Optimal allocation of DG unit for the radial distribution system using genetic algorithm," INTERNATIONAL JOURNAL OF INNOVATIVE RESEARCH IN ELECTRICAL, ELECTRONICS, INSTRUMENTATION

AND CONTROL ENGINEERING, Vol. 3, no 1, pp. 87-90, Jan, 2015.

[45] Ahmad Hassanat et al,"Choosing Mutation and Crossover Ratios for Genetic Algorithms—A Review with a New Dynamic Approach," Jornal of information, Vol.10, No.12, Nov 2019.

[46] D.B. Prakash, C. Lakshminarayana, "Multiple DG Placements in Distribution System for Power Loss Reduction Using PSO Algorithm," Procedia Technology, Vol. 25, pp.785 – 792, 2016.

[47] Heidari et al, "Harris hawks optimization: Algorithm and applications," Article in Future Generation Computer Systems, Vol. 97, pp. 849-872, March 2019.

[48] Omessaad Elbeji, Mouna Ben Hamed, Lassaad Sbita, "PMSG Wind Energy Conversion System: Modeling and Control," International Journal of Modern Nonlinear Theory and Application, Vol.3, pp. 88-97, July 2014.

[49] Rashmi.R, Ramanujan.V, Purushotham.M, "Permanent Magnet Synchronous Generator Configuration in Wind Turbines," International Journal of Scientific & Engineering Research, Vol. 6, no. 2, pp.23-31, February-2015.

[50] S. Soued1, H. S. Ramadan, M. Becherif, "Effect of Doubly Fed Induction Generator on Transient Stability Analysis under Fault Conditions," Energy Procedia, Vol. 162, pp.315–324, 2019.

[51] A. Dekhane et al, "DFIG Modeling and Control in a Wind Energy Conversion System," First International Conference on Renewable Energies and Vehicular Technology, pp.287-292, March 2012.

[52] Johan MORREN, Sjoerd W.H. de HAAN, "Maximum penetration level of distributed generation without violating voltage limits," Conference Paper, July 2008.

[53] Bindeshwar Singh, Bindu Jee Gyanis, "Impact assessment of DG in distribution systems from minimization of total real power loss view point by using optimal power flow algorithms, Energy Report, Vol. 4, pp. 407-417, 2018.

[54] Impacts and drivers of policies for electricity access Micro- and macro-economic analysis of Ethiopia's tariff reform,retrieved from, https://energyeconomicgrowth.org/node/236.

Appendix A

Appendix 1

A.1 Line and Load data of Sheno feeder

[Table A.1: Line and Load data of sheno feeder]

Line no	From bus	To bus	Resistance (ohm)	Reactance (ohm)	Real power (MW)	Reactive power (MVAr)
1.	1	2	0.3471	0.1936	0	0
2.	2	3	0.1446	0.2099	0.6758	0.5671
3.	3	4	0.1446	0.0695	0.2635	0.1224
4.	4	5	0.1157	0.0606	0.0450	0.0104
5.	5	6	0.0867	0.1035	0.0765	0.0311
6.	6	7	0.2314	0.1242	0.1700	0.1091
7.	7	8	0.2314	0.2390	0.1649	0.0982
8.	8	9	0.0578	0.0177	0.0607	0.0250
9.	9	10	0.1157	0.0311	0.0413	0.0240
10.	3	11	0.1157	0.1276	0.0675	0.0370
11.	11	12	0.0867	0.0644	0.0807	0.0384
12.	12	13	0.2314	0.1813	0.2000	0.1854
13.	13	14	0.0867	0.0783	0.03110	0.2590
14.	14	15	0.2603	0.1788	0.0842	0.0465
15.	15	16	0.1735	0.1478	0.0400	0.0127
16.	16	17	0.0289	0.0626	0.2669	0.1822

17.	17	18	0.0289	0.1641	0.6332	0.4218
18.	18	19	0.2578	0.1641	0.2603	0.1600
19.	19	20	0.1578	0.0714	0.1649	0.1186
20.	20	21	0.1778	0.0774	0.0453	0.0243
21.	21	22	0.2867	0.1774	0.5447	0.4132
22.	3	23	0.0867	0.0399	0.2644	0.1022
23.	23	24	0.3471	0.8277	0.2669	0.1246
24.	24	25	0.2314	0.1774	0.5525	0.2888
25.	25	26	0.0489	0.0227	0.1900	0.1340
26.	26	27	0.1735	0.2217	0.1755	0.0933
27.	27	28	0.1735	0.1299	0.0503	0.0132
28.	28	29	0.1446	0.1695	0.2100	0.1260
29.	29	30	0.1446	0.0340	0.6758	0.2494
30.	30	31	0.0867	0.1094	0.0713	0.0455
31.	31	32	0.0867	0.04035	0.0503	0.0241
32.	32	33	0.3471	0.2114	0.2669	0.1046
33.	23	34	0.1735	0.0576	0.2530	0.0838
34.	34	35	0.2314	0.1242	0.1159	0.0346
35.	35	36	0.1246	0.1091	0.0842	0.0476
36.	22	37	0.0578	0.0325	0.0913	0.0300
37.	37	38	0.1735	0.9607	0.1950	0.1580
38.	38	39	0.1446	0.0961	0.0605	0.0476
39.	39	40	0.2144	0.1537	0.1700	0.0976
40.					0.0882	0.0310

A.2 Wind turbine and DFIG Rating Parameter for the test system

Table A.2: Parameter of Nordex N80/2500 wind turbine

Parameter	Value(unit)
Rotor diameter	80 m
Hub height	80 m
Cut in speed	3 m/s
Cut out speed	25 m/s
Nominal wind speed	12.5 m/s
Speed range	9-16 rpm
Optimum TSR	7.2
Maximum power coefficient	0.44

Table A.3: DFIG Rating Parameter for the test system

Parameter	Value (unit)
Nominal stator active power	2 MW
Nominal torque	12.732 K.NM
Stator voltage	690 V
Nominal speed	1500 rpm
Speed range	900-200 rpm
Pole pair	2
Lm	2.5 *10ˆ-3H
Lr	87 *10ˆ-6
Ls	87 *10ˆ-6
Rr	0.026 ohm
Rs	0.029 ohm

A.3 Proposed Harris Hawks Optimization Code for optimal size and location of DG

```
% Harris's hawk optimization code for DG placement and sizing.
% T: maximum iterations, N: populatoin size
clear all
clc
close all
warning('off')
 N=30;
T=100;
```

```
UB=40; LB=2;
lb=1; ub=4;
dim=2;
disp('HHO is now tackling your problem')
tic
% initialize the location and Energy of the rabbit
Rabbit_Location=zeros(1,dim);
Rabbit_Energy=inf;
di=1;
%Initialize the locations of Harris' hawks
for run=2
for i=1:di
if size(UB,1)==1
    x(:,1)=ceil(rand(N,di).*(UB-LB)+LB);
    x(:,2)=round(rand(N,di).*(ub-lb)+lb,4);
end
if size(UB,1)>1
    for i=1:di
        high=UB(i);low=LB(i);
        HIGH=ub(i);LOW=lb(i);
        x(1,i)=ceil(rand(1,N).*(high-low)+low);
        x(2,i)=round(rand(1,N).*(HIGH-LOW)+LOW,4);
    end
end
end
[f]=Get_Functions_details(x,N);
B=f;
CNVG=zeros(1,T);
t=0; % Loop counter
while t<T
    for i=1:size(x,1)
        % Check boundries
```

```
FU=x(i,1)>UB;FL=x(i,1)<LB;x(i,1)=(x(i,1).*(~(FU+FL)))+UB.*FU+LB.*FL;
FU=x(i,2)>ub;FL=x(i,2)<lb;x(i,2)=(x(i,2).*(~(FU+FL)))+ub.*FU+lb.*FL;
    % fitness of locations
    fitness=B(i,:);
    % Update the location of Rabbit
    if fitness<Rabbit_Energy
        Rabbit_Energy=fitness;
        Rabbit_Location=x(i,:);
    end
end
E1=2*(1-(t/T)); % factor to show the decreaing energy of rabbit
% Update the location of Harris' hawks

    E0=2*rand()-1; %-1<E0<1
    Escaping_Energy=E1*(E0);  % escaping energy of rabbit
%         Escaping_Energy=0.1;
    if abs(Escaping_Energy)>=1
        %% Exploration:
        % Harris' hawks perch randomly based on 2 strategy:
        for i=1:N
        q=rand();
        rand_Hawk_index = floor(N*rand()+1);
        X_rand = x(rand_Hawk_index, :);
        if q<0.5
            % perch based on other family members
            X(i,:)=X_rand-rand()*abs(X_rand-2*rand()*x(i,:));
        elseif q>=0.5
% perch on a random tall tree (random site inside group's home range)
  X(i,:)=(Rabbit_Location(1,:)-mean(x))-rand()*((ub-lb)*rand+lb);
        end
        end
        [f]=Get_Functions_details(X,N);
```

```
            H=f;
             for i=1:N
    if H(i,:)<B(i,:) % improved move?
                    x(i,:)=X(i,:);
    end
             end

        elseif abs(Escaping_Energy)<1
            %% Exploitation:
            r=rand(); % probablity of each even
            if r>=0.5 && abs(Escaping_Energy)<0.5 % Hard besiege
                for i=1:N
     X(i,:)=(Rabbit_Location)-Escaping_Energy*abs(Rabbit_Location-x(i,:));
                end
            end
            [f]=Get_Functions_details(X,N);
            H=f;
             for i=1:N
    if H(i,:)<B(i,:) % improved move?
                    x(i,:)=X(i,:);

                end

             end

            if r>=0.5 && abs(Escaping_Energy)>=0.5  % Soft besiege
   for i=1:N
Jump_strength=2*(1-rand()); % random jump strength of the rabbit
X(i,:)=(Rabbit_Location-x(i,:))-Escaping_Energy*abs...
     (Jump_strength*Rabbit_Location-x(i,:));
                end
            [f]=Get_Functions_details(X,N);
```

```
        H=f;
          for i=1:N
if H(i,:)<B(i,:) % improved move?
                    x(i,:)=X(i,:);

              end

          end
[f]=Get_Functions_details(x,N);
  s=f;
  for i=1:size(x,1)
   % fitness of locations
    fitness=s(i,:);
    % Update the location of Rabbit
    if fitness<Rabbit_Energy
        Rabbit_Energy=fitness;
        Rabbit_Location=x(i,:);
    end
  end

        end
       %% phase 2: performing team rapid dives (leapfrog movements)
        if r<0.5 && abs(Escaping_Energy)>=0.5,

            Jump_strength=2*(1-rand());
            for i=N
       X1=Rabbit_Location-Escaping_Energy*abs...
           (Jump_strength*Rabbit_Location-x(i,:));
        [f]=Get_Functions_details(X1,N);
        H=f;
if H<B(i,:) % improved move?
                    x(i,:)=X1;
```

```
                else
                        [o]=levy(dim);
    X2=Rabbit_Location-Escaping_Energy*abs...
        (Jump_strength*Rabbit_Location-x(i,:))+rand(1,dim).*o;
         [f]=Get_Functions_details(X2,N);
         R=f;
if R<B(i,:) % improved move?
                    x(i,:)=X2;
end
end
          end
         end
             if r<0.5 && abs(Escaping_Energy)<0.5,
                 Jump_strength=2*(1-rand());
              for i=N

       X1=Rabbit_Location-Escaping_Energy*abs...
           (Jump_strength*Rabbit_Location-mean(x));
         [f]=Get_Functions_details(X1,N);
         H=f;
if H<B(i,:) % improved move?
                    x(i,:)=X1;
                else
                    [o]=levy(dim);
    X2=Rabbit_Location-Escaping_Energy*abs...
        (Jump_strength*Rabbit_Location-mean(x))+rand(1,dim).*o;
if R<B(i,:) % improved move?
                    x(i,:)=X2;
end
end
          end
         end
```

```
        [f]=Get_Functions_details(x,N);
        s=f;
        for i=1:N
         % fitness of locations
          fitness=s(i,:);
          % Update the location of Rabbit
          if fitness<Rabbit_Energy
               Rabbit_Energy=fitness;
               Rabbit_Location=x(i,:);
          end
        end
              end
           t=t+1;
    CNVG(t)=Rabbit_Energy;
end
r=Rabbit_Energy;
R=Rabbit_Location;
if Rabbit_Energy<r
     r=Rabbit_Energy;
     R=Rabbit_Location;
end
end
toc
figure,
hold on
semilogy(CNVG,'Color','b','LineWidth',4);
title('Convergence curve')
xlabel('Iteration');
ylabel('Best fitness obtained so far');
axis tight
grid off
box on
```

```
legend('HHO')
display(['The best location of HHO is: ', num2str(R)]);
display(['The best fitness of HHO is: ', num2str(r)]);
```